SPECIAL ISSUE PAPER

WILEY

Investigating the impacts of biochar on water fluxes in a rice experiment in the dry corridor of Central America, Costa Rica

Benjamin M. C. Fischer[1,2,3] | Laura Morillas[4] | Johanna Rojas Conejo[5] | Ricardo Sánchez-Murillo[6] | Andrea Suárez Serrano[5] | Jay Frentress[7,8] | Chih-Hsin Cheng[9] | Monica Garcia[10] | Stefano Manzoni[1,3] | Mark S. Johnson[11,12] | Steve W. Lyon[1,3,13]

[1]Department of Physical Geography, Stockholm University, Stockholm, Sweden

[2]Department of Earth Sciences, Uppsala University, Uppsala, Sweden

[3]Bolin Centre for Climate Research, Stockholm University, Stockholm, Sweden

[4]Centre for Sustainable Food Systems, The University of British Columbia, Vancouver, Canada

[5]Water Resources Center for Central America and the Caribbean (HIDROCEC-UNA), Universidad Nacional de Costa Rica, Heredia, Costa Rica

[6]Department of Earth and Environmental Sciences, University of Texas, 500 Yates St, Arlington, Texas, 76019

[7]Faculty of Science and Technology, Free University of Bolzano, Italy

[8]Water Resources, Ramboll Sverige AB, Stockholm, Sweden

[9]School of Forestry and Resource Conservation, National Taiwan University, Taipei, Taiwan

[10]Research Centre for the Management of Agricultural and Environmental Risks (CEIGRAM), E.T.S.I. Agronomica, Alimentaria y de Biosistemas, Universidad Politécnica de Madrid, Madrid, Spain

[11]Department of Earth, Ocean and Atmospheric Sciences, The University of British Columbia, Vancouver, Canada

[12]Institute for Resources, Environment and Sustainability, The University of British Columbia, Vancouver, Canada

[13]School of Environment and Natural Resources, Ohio State University, Columbus, Ohio, USA

Correspondence
Benjamin M. C. Fischer, Department of Physical Geography, Stockholm University, Stockholm, Sweden.
Email: benjamin.fischer@natgeo.su.se

Abstract

Amending soils with biochar, a pyrolyzed organic material, is an emerging practice to potentially increase plant available water and reduce the risks associated with climatic variability in traditionally-rainfed tropical agricultural systems. To investigate the impacts of biochar amendment on soil water storage relative to non-amended soils, we performed an upland rice field experiment in a tropical seasonally dry region of Costa Rica consisting of plots with two different biochar amendments and a control plot. Across all plots, we collected hydrometric and isotopic data (δ^{18}O and δ^{2}H of rain, mobile soil, ground and rice xylem water). We observed that the soil water retention curves for biochar treated soils shifted, indicating that rice plants had 2% to 7% more water available throughout the growing season relative to the control plots and thus could withstand dry spells up to seven extra days. Furthermore, the isotopic composition of plant water in biochar and control treatments were rather similar, indicating that rice plants in different treatments likely consumed similar water.

Hence, we observed that biochar amendments can stabilize water supplies for the rice plants; however, still supplemental irrigation was required to facilitate plant growth during extended dry periods. Ultimately, our findings indicate, that biochar amendments can complement, but not necessarily replace, other water management strategies to help reduce the threat of rainfall variability to rainfed agriculture in tropical regions.

1 | INTRODUCTION

Rainfed agriculture provides food for the growing world population (de Fraiture et al., 2009; de Fraiture and Wichelns, 2010) without over-exploiting groundwater resources (Famiglietti, 2014; Jasechko et al., 2017). However, the spatial and temporal variability of rainfall makes rainfed agriculture vulnerable to droughts (Fischer et al., 2013) and poses a risk to food security (de Fraiture & Wichelns, 2010). Weather phenomena such as El Niño-Southern Oscillation (ENSO) influence global precipitation patterns and can bring prolonged dry spells that limit rainfed agriculture production. This is especially true in the tropics, where rainfall regimes will continue to change (Feng et al., 2013; Giorgi, 2006; Knutson et al., 2006), leading to more frequent long-term droughts (e.g. sustained droughts with a periodicity of around 10 years are expected in the Central America Dry Corridor; Hidalgo et al., 2019). For example, climate projections for the Mesoamerican tropics suggest (1) decreases in rainfall during the wet season (May–November) of 10% to 25%; (2) expansion of the areas affected by mid-summer droughts; and (3) increases in temperature and extreme dry spells. Collectively, these changes will result in a net decrease in water availability (Imbach et al., 2018), which could have significant impacts on rainfed agricultural production and food security globally. Therefore, to reduce societal exposure to risk, it becomes necessary to make rainfed agriculture more resilient to current and future climate variability.

Agricultural innovations can offer a pathway forward. Many innovative water management strategies have been put forward capturing rain (Biazin et al., 2012) or flood water (Castelli et al., 2018), adopting plant and soil water conservation measures (Enfors & Gordon, 2007; Makurira et al., 2007; Vico & Brunsell, 2018) or introducing supplementary irrigation (Mutiro et al., 2006). Amending soils with biochar is an emerging practice in agriculture that could be useful to improve agricultural resilience to climate variability (Fischer et al., 2018). Biochar is a collective name for organic material (e.g., woody or herbaceous vegetation, crop residues, or waste material) that is pyrolyzed in low-tech (Sundberg et al., 2020) or high-tech furnaces (Liu et al., 2016). The result is a charcoal with different material properties (e.g., particle size, pore structure, surface area, and hydrophobicity) from the original feedstock. Biochar can be applied on the soil surface or incorporated in the soil where it alters the original soil matrix, thereby changing the infiltration capacity (Blanco-Canqui, 2017; Lim & Spokas, 2018; Sun & Lu, 2014) and creating a multilayer soil profile, that is, a soil layer amended with biochar and layers of soils without biochar amendments. The altered soil physical characteristics increase the soil water holding capacity and the amount of soil water stored at a given soil matric potential in general (Omondi et al., 2016; Oppong Danso et al., 2019). Biochar often is seen to bring about an increase in agricultural productivity; however, despite the documented positive effects of biochar amendments on agricultural productivity (Kätterer et al., 2019; Novak et al., 2016), several cases of negligible or limited effects have also been observed (Fischer et al., 2018; Jeffery et al., 2015, 2017; Nelissen et al., 2015; Reyes-Cabrera et al., 2017). These diverging findings might be due in part to different biochar typologies (Fischer et al., 2018), but can also be attributed emphasis of, studies on laboratory and pot experiments that are likely unable to mimic the variety of processes occurring in agroecosystems at the field and agroecosystems scales (Agegnehu et al., 2017; Blanco-Canqui, 2017; Zhang et al., 2016). At the agroecosystem scale, soil water depends not only on the storage characteristics of the soil but also on the variability of vertical water fluxes resulting from rainfall and irrigation, evaporation, leakage, and runoff (Falkenmark, 1997; Rockström, 1999; Vico & Porporato, 2015). Thus, biochar impacts could manifest themselves to varying extents across the myriad pathways by which water can move through the soil–plant-atmosphere continuum.

To help assess the impacts of biochar, across this continuum, it may prove useful to consider the composition of the relative pools of water through the use of tracers. For example, stable isotopes of the water (^{18}O and ^2H) in combination with hydrometric data offer a proven tool to trace water from rainfall to the catchment outlet (Fischer et al., 2017; Klaus & McDonnell, 2013). Typically, tracing water in this fashion is done by characterizing differences or similarities concerning the spatiotemporal rainwater (Fischer et al., 2018), water fluxes through evaporation (Benettin et al., 2018; Gonfiantini, 1986), water from the (un)saturated zone or groundwater (Jasechko et al., 2017; Koeniger et al., 2016; Sánchez-Murillo & Birkel, 2016; Saxena, 1987). The isotopic composition of extracted plant xylem water is then often considered to trace the water within the soil–plant-atmosphere continuum of natural systems and help to identify which pools of water plants are consuming water from (Allen
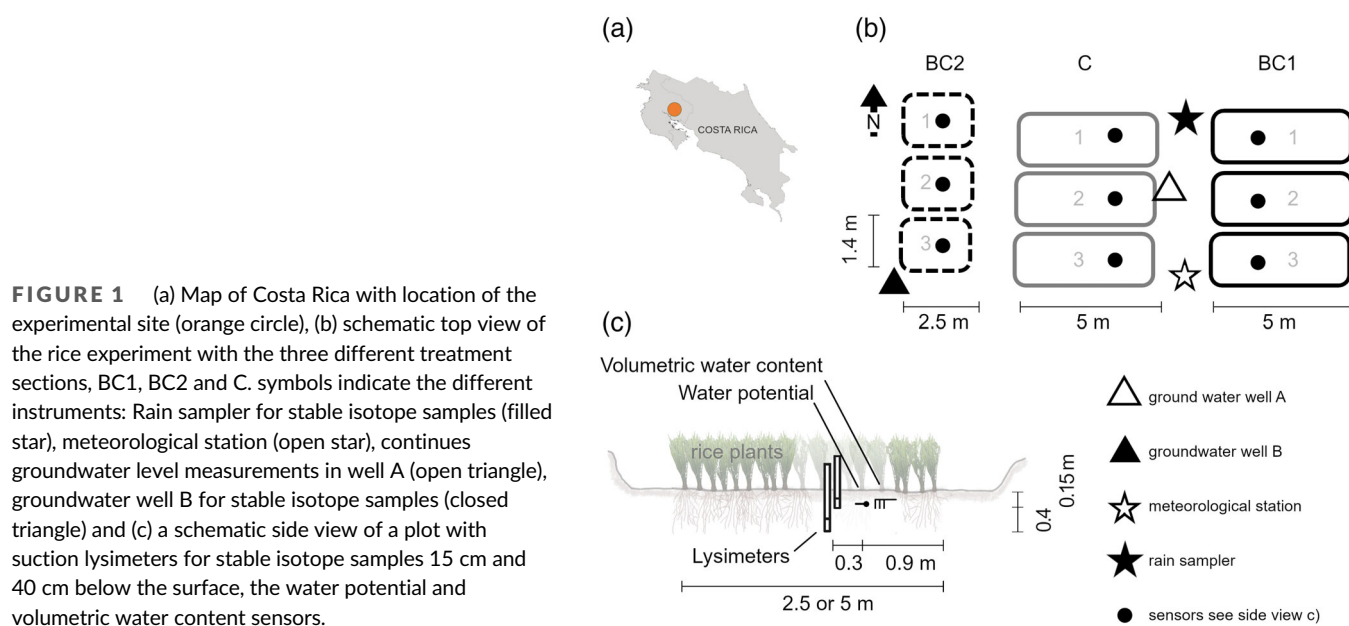
et al., 2019; Brooks et al., 2010; Dawson & Ehleringer, 1991; McDonnell, 2014; Penna et al., 2018; Rothfuss & Javaux, 2017; Sprenger et al., 2016). Even without explicitly tracing the source or flux of water through the soil–plant-atmosphere continuum, stable water isotopes can potentially offer insights to characterize the pools of water that exist in a landscape in terms of similarities and differences (Sánchez-Murillo, Esquivel-Hernández, Birkel, et al., 2020). While stable water isotopes are now a proven method to study natural systems, they have seen limited application in agricultural systems (Penna et al., 2020) with exceptions (i.e., in coffee (Muñoz-Villers et al., 2020), maize, wheat (Stumpp et al., 2009) and rice cultures (Mahindawansha et al., 2018; Sheng & Zhu, 2018)) and biochar field experiments even less (i.e., Lyon et al. (2022)).

Despite biochar's potential promise as a water management tool for rainfed agriculture, (Fischer et al., 2018) pointed out discrepancies between empirical field evidence of how biochar affects water fluxes and suggestions that biochar additions make tropical agriculture more resilient to climate variability. Here we leverage hydrometric data in combination with stable isotopes to study the complex interactions between water fluxes and storages that determine the potential implications of amending soils with biochar as an agricultural innovation to deal with current and potential future climatic variability. Specifically, we performed a field experiment with upland rice in soil amended with two different biochar types vs. a control treatment (no biochar) in a tropical seasonally dry region in northwestern Costa Rica. We use a combination of hydrometric and isotopic data ($\delta^{18}O$ and δ^2H of rain, mobile soil, ground, and rice plant water) to assess (1) the extent to which biochar amendments increase soil water storage relative to non-amended soils during the rice growing period, and (2) if rice plants grown in biochar amended soils have a different stable isotopic composition of water compared to those grown in non-amended soils indicating that rice plants access different pools of water.

2 | STUDY SITE AND EXPERIMENTAL DESIGN

2.1 | Study site

The biochar rice experiment was conducted at the Enrique Jímenez Núñez Experimental Station (EEEJN) from the Instituto Nacional de Innovación y Transferencia en Tecnología Agropecuaria (INTA) near the city of Cañas in the Guanacaste province of Costa Rica (Figure 1a). Soils at the experimental site are loamy vertosols (Table A1) typically more than 2 m deep (Diogenes Cubero & Maria José Elizondo, 2014). Guanacaste province is part of the Dry Corridor of Central America (Sánchez-Murillo, Esquivel-Hernández, Corrales-Salazar, et al., 2020) and is characterized by a seasonally dry tropical climate with marked dry and wet seasons and limited temperature variability over a year (Birkel et al., 2017). The annual average temperature at EEEJN-INTA is 27.4°C. The dry season typically spans from mid-November to April with virtually no rainfall. Wet season precipitation exhibits a bi-modal distribution dominated by the influence of the Intertropical Convergence Zone with peaks occurring in May/June and September/October. The moderate dry period between these two peaks is usually referred to as the mid-summer drought (Magaña et al., 1999). The average annual rainfall in the area is approximately 1547 ± 473 mm yr^{-1} based on a 100-year observation record from a meteorological station ∼10 km distance from the experimental site (Figure 2a). The annual average actual evapotranspiration is around 1100 mm yr^{-1} (Sánchez-Murillo & Birkel, 2016). In the last century, 70% of the driest years in this region (i.e., years with less than 1153 mm yr^{-1} of rainfall, which is the 25th percentile of annual rainfall), occurred during warm ENSO years. Based on the Standardized Precipitation Index (SPI; Narseh Kumar et al., 2009), recurrent below-average rainfall has been observed in this region since the 1960s

FIGURE 1 (a) Map of Costa Rica with location of the experimental site (orange circle), (b) schematic top view of the rice experiment with the three different treatment sections, BC1, BC2 and C. symbols indicate the different instruments: Rain sampler for stable isotope samples (filled star), meteorological station (open star), continues groundwater level measurements in well A (open triangle), groundwater well B for stable isotope samples (closed triangle) and (c) a schematic side view of a plot with suction lysimeters for stable isotope samples 15 cm and 40 cm below the surface, the water potential and volumetric water content sensors.
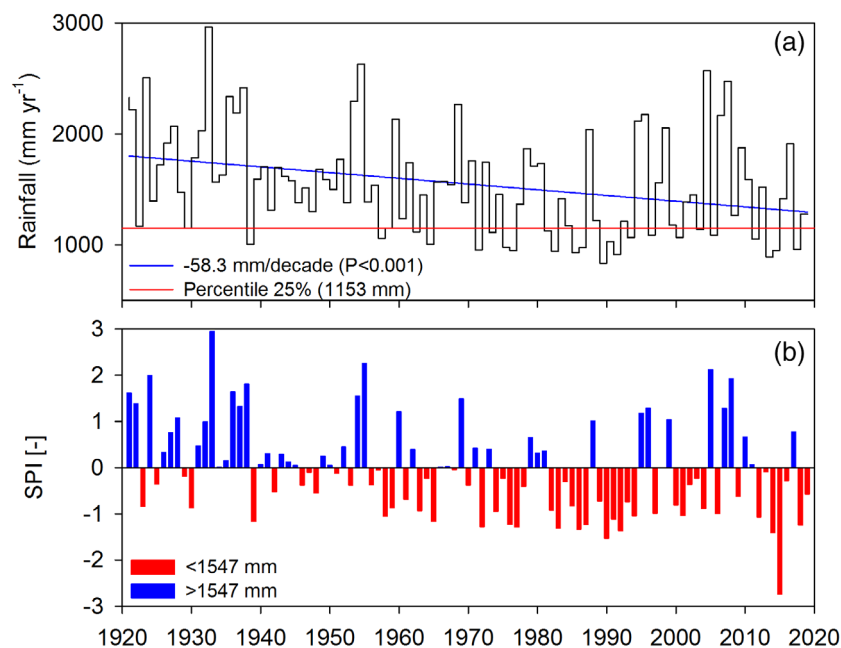
FIGURE 2 (a) Long-term rainfall (mm yr^{-1}) including a significant rainfall decrease of 53 mm per decade (blue line) and 25% percentile of 1153 mm (red line as reference) and (b) standardized precipitation index (SPI) within the lowlands of Guanacaste between 1921 and 2019 (long-term rainfall average = 1547 ± 473 mm yr^{-1}; rainfall data source: Ing. Werner Hagnauer, Cañas, Guanacaste).

(Figure 2b) with a significant periodicity of severe (SPI < −1.5) and sustained droughts of around 10 years (Hidalgo et al., 2019).

2.2 | Experimental design

For this experiment two types of biochar were tested to represent a more locally-produced biochar and a more industrially-processed biochar, respectively. Biochar 1 (BC1) was made of locally-sourced bamboo (*Guadua Angustifolia*) and produced at the Costa Rica Institute of Technology (TEC, Cartago, CR; Table A1). The feedstock consisted of wood pieces up to 30 cm in length from construction waste, which were pyrolyzed using a pyrolysis furnace under a temperature ranging from 450 to 480°C. A second biochar, biochar 2 (BC2) was produced from sugarcane filter cake collected from the Huwei Sugar Mill (Taiwan Sugar Corporation, Taipei, Taiwan). For the industrial processing of BC2, the filter cake was pelletized into pellets of 7.6 mm diameter and 20–30 mm long and pyrolyzed at 600°C under a controlled nitrogen-rich atmosphere. Pyrolyzed pellets were crushed and sieved to ≤2 mm prior to field application.

Within the EEEJN-INTA experimental station, an area of approximately 100 m^2 was available where biochar BC1 was incorporated into the field for an irrigated melon crop experiment during the dry season (Lyon et al., 2022) about 6 months before the start of this study. The area contained two different treatment sections, one containing biochar type BC1 and a control treatment (C) with no biochar added. The treatments were subdivided into three plots each to create three independent monitoring replicates of each treatment (Figure 1b). The BC1 and C plots were 7 m^2 each (5 m long × 1.4 m wide) in area. To perform our rice experiment, the experimental area was extended with 60 m^2 (total area of 160 m^2). Due to a lower amount of BC2 being available (shortage of feedstock at the biochar supplier) while securing a similar application rate (1 kg m^{-2}) across

biochar treatments the BC2 plots were 3.5 m^2 each (2.5 m long × 1.4 m wide) in area. Similar to the BC1 plots the biochar with particle size ≤2 mm particle was mechanically worked into the top 20 cm of the field prior to planting.

After the treatment sections were prepared, an upland rice variety Palmar 18 (*Oryza Sativa* L.) was sown (1 seed cm^{-1}, ∼ 20 g m^{-2}, 5 cm deep longitudinal rills, 25 cm spacing) simultaneously on the three sections on 18 July 2018 indicating the start of the experiment. During the growing season, rice plants were primarily rainfed which is the standard procedure for the predominant upland rice grown in the region. In some cases, where water sources for irrigation are available, sporadic support irrigation is used by local farmers to support crops and avoid wither. Due to prolonged dry spells that occurred during the study period, all experimental plots were irrigated with 7 L m^{-2} water from an irrigation canal with origin from the mountains on July 22 and August 25 to assist germination and avoid plant drought damage, respectively, on each date. Following typical regional crop management practices, fertilizer (100 g m^{-2} consisting of 10% N, 30% P, 10% K in combination with 11 ml MEGAFOL® and 11 g magnesium sulphate) and insecticide/herbicide (2 ml Muralla® Delta; 50 ml Garlon and 20 ml bispiribac sodium) were applied to all experimental plots using 2 L m^{-2} irrigation water on each treatment date (August 10, September 6 and November 5) to support plant growth. At monthly intervals, manual weed control was performed in all plots. Harvest took place on 21 November 2018 and indicated the end of the experiment.

2.3 | Instrumentation and sampling

2.3.1 | Meteorological and hydrometric observations

A meteorological station (Vaisala WT520; 1.5 m height) was used to continuously monitor precipitation, wind speed and direction, air

temperature, relative humidity, and atmospheric pressure at the site during the entire study period (Figure 1b,c). Each experimental plot was instrumented with one sensor installed at 15 cm depth to monitor volumetric soil water content, soil electrical conductivity, and soil temperature (model GS3, Decagon Devices, Inc., Pullman USA), and one additional sensor at the same depth to monitor soil matric potential and soil temperature (model MPS6, Decagon Devices). Both sensors were placed between rice rows in each plot (Figure 1c). Additionally, soil samples were collected at 15 cm soil depth from each plot at the beginning of the experiment and after harvest to determine the gravimetric soil moisture content and used for a two-point calibration of the continuous volumetric soil water content measurements.

Depth of groundwater levels was measured using a groundwater well (groundwater well A) installed between the BC1 and C treatment sections (Figure 1b). The well consisted of screened PVC tube instrumented with a sensor to continuously monitor groundwater level, electrical conductivity, and water temperature (model CTD, Decagon Devices). Manual water level measurements were made every other week during the study period to calibrate the continuous water level measurements. All sensors were connected to a data logger (Campbell CR1000 logger and an AM416 Relay Multiplexer) and programmed to record at 30-minute intervals.

2.3.2 | Water and plant sample collection

Water samples from different pools of water were collected for isotopic analysis. Rainwater was collected using a funnel connected with tubing to a PET bottle (1.5 litre) wrapped in aluminium foil similar to Prechsl et al. (2014). In each plot, suction lysimeters (Soilmoisture equipment corp., Santa Barbara, USA) were installed in the soil reaching to 15 and 40 cm soil depth respectively to sample soil water (the so-called mobile soil water). Groundwater samples were collected from a second groundwater well (groundwater well B) installed near the BC2 treatment section (Figure 1b).

Rainwater samples were collected daily at 7:00 AM. Water from additional application sources such as irrigation (to supplement rainfall) and fertilizer/pesticide/herbicide applications were sampled as a grab sample using a PE bottle during each application. Soil water and groundwater samples were collected approximately biweekly (every other week) after plant germination from 31 July 2018 until the harvest day on 21 November 2018, resulting in 11 sampling days. At approximately 9:00 AM on each sampling day, each suction lysimeter had a vacuum of 800-mbar applied for 1 hour. After releasing the vacuum of each suction lysimeter, on average 100 ml of soil water was collected. Groundwater was sampled by purging the well and waiting 1 hour before collecting the groundwater sample. The different soil and groundwater samples were collected in 30 ml PE bottles, which were capped and sealed with Parafilm® for transport and cold storage (5°C) until analysis. At the end of each sampling day, all excess water from all sampler tubing, bottles, and suction lysimeters was removed to prevent inter-sampling contamination.

In addition to the mobile soil water, soil samples were collected randomly in all plots from a depth of 5–10 cm on 7 out of 11 sampling days for bulk soil water (mobile and immobile soil water) extraction and subsequent stable isotope analysis. To not disturb the rice plants, instead of an auger, a soil corer 50 cm in length with a 2 cm diameter was pushed 10 cm into the soil. After removing 5 cm of the topsoil, the soil sample of about 60 cm^3 was collected and placed in a double re-sealable zipper storage bag. To minimize post-sampling evaporation, the storage bags were directly placed in a cooler with ice. All soil samples were stored in the laboratory freezer (−80 C) before extracting the bulk soil water for isotopic analysis.

Plant material from the rice plants was collected on each of the 11 biweekly sampling dates at around noon. For plant material sampling, six rice plants (until 21 September) and three rice plants (from 12 October until harvest) were randomly selected within each plot. The plant height from the soil to the plant tip was measured and recorded before sampling. To avoid loss of biomass on sampled plants, the plants were extracted using a small knife which was carefully wiggled into the soil to extract the rice plant and as much of the root network without disturbing neighbouring plants. The roots and stems of the extracted plants were separated immediately and transferred into double re-sealable zipper storage bags. The roots (∼5–10 cm) were carefully ticked with fingers to remove the stuck dry soil. To minimize post-sampling transpiration, storage bags were directly placed in a cooler with ice. All plant material was stored in the laboratory freezer (−80°C) before extracting the plant water for isotopic analysis.

3 | LABORATORY METHODS AND DATA ANALYSIS

3.1 | Plant and bulk soil water extraction

Xylem water was extracted from the stem of the different rice plants to infer which sources of water the rice plants used. We used the cryogenic vacuum extraction technique described by Koeniger et al. (2011) to extract the plant and bulk soil water for stable isotope analysis. About 3 g of plant material from the rice stem was placed in the heated vial before the system was evacuated to 85 kPa with a hand vacuum pump (Mityvac). The heated vial was heated for 1 hour at 100°C using a test tube heater (HI839800 COD Test Tube Heater; Hanna instruments) while the cold trap vial rested in a Dewar flask containing liquid nitrogen at about −196°C. After the extraction was stopped, the cold trap vial was sealed with Parafilm and left to thaw. After thawing, the extracted liquid water was pipetted into 2 ml vials (32 × 11.6 mm screw neck vials with cap and PTFE/silicone/PTFE septa) and stored refrigerated (5°C) until stable isotope analysis. The plant root and bulk soil water were extracted in the same manner as the xylem water using the cryogenic vacuum extraction technique but with extraction times longer than 3 hours. On average 86 ± 5% xylem water was extracted. However, we could extract less than 0.1 ml of water per plant root and soil sample. These volumes of water were too small for pipetting and the subsequent isotopic analysis.

3.2 | Isotope analysis

All non-plant water samples were filtered (0.45 μm filter 13 mm PTFE Syringe Filter, Fisher scientific) and pipetted in vials (2 ml into a 1.5 ml 32 × 11.6 mm screw neck vials with cap and PTFE/silicone/PTFE septa) prior to analysis. Water stable isotope analysis was conducted at the Stable Isotopes Research Group facilities of the Universidad Nacional of Costa Rica using a water isotope analyser LWIA-45P (Los Gatos Research Inc., USA). All data were normalized to the VSMOW-SLAP scale (Vienna Standard Mean Ocean Water- Standard Light Antarctic Precipitation scale, [IAEA, 2009]) and corrected for drift and memory effects following the procedure of Sánchez-Murillo and Birkel (2016). The analytical long-term error was ±0.5 (‰) (1σ) for δ^2H and ± 0.1 (‰) (1σ) for δ^{18}O.

The xylem water stable isotopes analysis was conducted at the Swedish University of Agricultural Sciences (SLU) Stable Isotope Laboratory (SSIL) in Umeå using an Isotope Ratio Mass Spectrometer (TC/EA-IRMS; DeltaV Advantage, Thermo Fisher Scientific, Bremen, Germany; High-Temperature Conversion Elemental Analyser, Thermo Fisher Scientific, Bremen, Germany and an AI 1310 Autosampler, Thermo Fisher Scientific, Bremen, Germany). All water samples were injected into a glassy carbon reactor containing glassy carbon chips at 1400°C and converted to H_2 and CO gases which were separated on a column and analysed on a mass spectrometer. All data were corrected for drift and memory. The analytical precision and accuracy were ± 2 (‰) (1σ) for δ^2H and ± 0.15 (‰) (1σ) for δ^{18}O.

All stable isotope compositions are presented as delta notations (δ) in ‰, relating the ratios (R) of ^{18}O/^{16}O and ^{2}H/^{1}H, relative to the VSMOW-SLAP scale. In addition, the deuterium excess (d-excess) was defined as $d\text{-}excess = \delta^2H – 8 \cdot \delta^{18}O$ (Dansgaard, 1964).

3.3 | Evapotranspiration and soil water retention impacts

Daily evapotranspiration rates (ET) from the experimental area were estimated by the crop coefficient method ($ET = K_c \cdot ET_{ref}$), a.k.a. FAO56 Penman-Monteith method (Allen et al., 1998). We used site-specific meteorological observations to estimate daily reference ET (ET_{ref}) and experimentally derived crop coefficient (K_c) values for the three different stages of crop growth (initial, mid-season, and late-season). Instead of using globally averaged values of K_c for rice (Allen et al., 1998), we used region-specific K_c values experimentally derived from a nearby field experimental site equipped with an Eddy Covariance (EC) tower where the same variety of upland rice was grown (Morillas et al., 2019). Daily K_c values from the EC site were derived as the ratio of daily measured ET and site-specific ET_{ref}, and then averaged for the three crop growth stages (K_c initial = 0.7, K_c mid-season = 0.9 and K_c late-season = 0.5). The length of each crop growth stage was calibrated for this region by observing the pattern of daily measured ET over the whole growing season (initial ≈ 25 days, development ≈ 20 days, mid-season ≈ 50 days, late-season ≈ 23 days for an average growing season of 120 days).

Field derived 30-min records of all meteorological and hydrometric observations were aggregated to daily averages. Accumulated precipitation and evapotranspiration were derived from daily measurements and estimates respectively for the entire experimental period (July 18–November 21). Average volumetric soil water content and soil matric potential for each treatment (BC1, BC2 and C) were calculated by averaging the observations in the three replicated plots per treatment.

Treatment specific volumetric soil water content (θ) and soil matric potential (ψ) were linked through soil water retention curves using the Van Genuchten model (Van Genuchten, 1980) (Equation (1))

$$\theta = \theta_r + \frac{\theta_s - \theta_r}{\left[1 + (\alpha\psi)^n\right]^m} \tag{1}$$

where θ_r [%], α [−] and n [−] represent residual soil water content, and the fitted scale and shape parameters, respectively; and $m = 1 − 1/n$ [−]. Saturation soil water content (θ_s) was based on field average daily observations while θ_r, α and n were estimated using the nonlinear data-fitting function in Matlab 2019 (MathWorks, USA). To examine the effect of biochar on soil physical and hydraulic properties, we compared the indicators soil water content at wilting point (θ_{WP}), soil water content at field capacity (θ_{FC}), and van Genuchten parameters α and n estimated for the biochar amended (BC1 and BC2) and for the unamended (C) treatments using response ratios (RR) as in Fischer et al. (2018). For this study, RR represents the ratio of the variable of interest in the treatment to the same property in the control such that RR >1 or RR <1 indicates that the treatment has a positive or negative effect, respectively.

3.4 | Isotope data analysis

The isotopic composition of the water samples was represented as collected in time. The within-treatment variability defined as difference between the minimum and maximum observed isotopic composition of plant water within a treatment on any given sampling day were calculated and presented as box plots. In addition, isotopic composition of the different water samples was represented in the dual isotope space δ^{18}O and δ^2H. The Global Meteoric Water Line (GMWL) was defined as $\delta^2H = 8 \cdot \delta^{18}O + 10$ by Craig (1961). The Local Meteoric Water Line (LMWL) was derived as $\delta^2H = 7.4 \cdot \delta^{18}O + 5.5$ using the long-term isotopic data from the rain sampler at the Water Resources Center for Central America and the Caribbean located ~50 km distance of the experimental site (Sánchez-Murillo, Esquivel-Hernández, Birkel, et al., 2020).

4 | RESULTS

4.1 | Temporal variability of precipitation, evaporation, soil moisture, groundwater and plant growth observed in the different experimental plots

Based on the temporal variability of rainfall, we identified three distinct periods within the overall study period (Figure 3). Period I

FIGURE 3 Time series of (a) rice plant average height (H_{plant}, filled green circles and dashed line) and the standard deviation the plant height (open black circles); (b) precipitation (P, black bars), estimated evapotranspiration (ET, solid orange line), accumulated P (solid black line) and accumulated ET (orange dashed line). The water sampling days 1–11 are indicated in each panel as vertical dashed lines and numbered on top of panel a and the date are given on the x-axis of panel b as dd.Mm. Periods I, II and III are indicated on the top of panel a. Time series of: (c) average volumetric water content and (d) average water potential for each treatment; (e) measured groundwater level. The different water sampling days 1–11 are indicated in each panel as vertical dashed lines and numbered on top of panel c and the date are given on the x-axis of panel e as dd. mm. Periods I, II and III are indicated on the top of panel c.
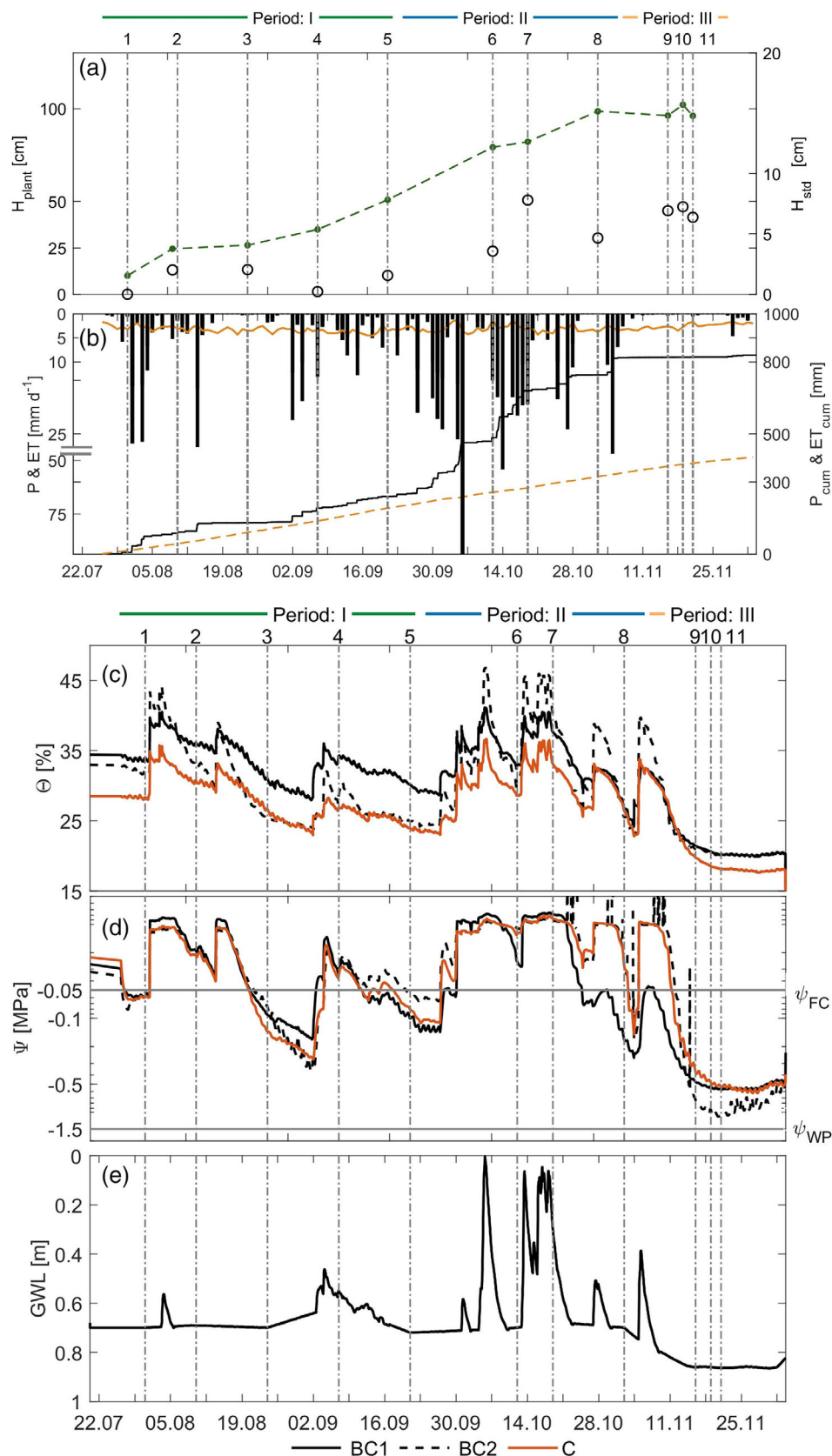
(18 July to 20 September) was characterized by alternating wet and dry days, Period II (20 September to 9 November) presented consistent high daily rainfall inputs, and Period III (10 November to 21 November) was characterized by a long dry spell ending with the rice harvest. Throughout the study period, daytime air temperatures were around 26.7°C (standard deviation $S_D = 3$°C),

and evapotranspiration rates on average 3.1 mm day^{-1} ($S_D = 0.7$ mm day^{-1}).

During Period I (germination and vegetative phase), the rice in the different plots grew to a height of 50 cm in all experimental plots (S_D <2.5 cm). This period was characterized by intermittent dry and wet spells with accumulated precipitation slightly higher than evapotranspiration ($P_{cum} = 240$ mm and $ET_{cum} = 191$ mm over the 64-day period; Figure 3b). During this period, the maximum recorded volumetric soil water contents were 40%, 43% and 35%, and the minimum values were 30%, 25% and 23% in the BC1, BC2, and control treatment, respectively (Figure 3c). Soil matric potential (ψ) was higher than field capacity ($\psi_{FC} = -0.05$ MPa) during rain events, with a maximum of -0.008 MPa and decreased to a minimum of -0.32 MPa (above the wilting point, $\psi_{WP} = -1.5$ MPa), observed in all treatments a few days after the third sampling day during the driest spell of Period I (Figure 3d). Generally, the soil matric potential in the biochar treatments was 0.002 MPa higher than in the control treatment. The groundwater level was generally 0.7 m below the surface and rose to less than 0.5 m below the surface in response to the highest rainfall of Period I (Figure 3e).

During Period II (vegetative and reproductive phase), rice plants attained their maximum heights of around 100 cm (S_D <5 cm), across all three plots. Period II was the wettest period with 15 out of 42 rain days with intensities greater than 20 mm d^{-1} of rainfall and 1 day with 93 mm d^{-1} (Figure 3a,b). Cumulative precipitation was therefore higher than cumulative evapotranspiration during the 50-day period ($P_{cum} = 570$ mm and $ET_{cum} = 147$ mm). The volumetric soil water content over Period II was generally higher than in Period I, with multiple peaks driven by rainfall events and then a decrease towards the end of the period. After rain events, the volumetric soil water contents rose from 28% to 40%, from 24% to 45%, and from 23% to 36% in BC1, BC2, and control treatment, respectively. Soil moisture then decreased in the three treatments to 28%, 25% and 24% during the last part of the period. The soil matric potential during Period II remained largely above field capacity except by the end of the period when it decreased (before sampling day 8) to a minimum of -0.23 MPa in BC1 and -0.16 MPa in BC2 and C. The groundwater level increased multiple times during this period from 0.7 m below the surface to reach the soil surface on the rainiest day of the study period.

During the final experimental period, Period III (ripening phase), rice plants maintained their maximum height acquired by the end of Period II. This period was characterized by a 12-day long dry spell such that cumulative evapotranspiration was greater than cumulative precipitation ($P_{cum} = 2$ mm and $ET_{cum} = 63$ mm over the 12-day period). By the end of Period III, the volumetric soil water content in the BC1 and BC2 treatments converged to the lowest observed value of ~21%. The control treatment reached this value about 7 days earlier than the biochar amended plots, and the control plots continued drying to reach a minimum value of 18% (Figure 3c). The soil matric potential for all three plots decreased from above the field capacity to near the wilting point by the end of Period III. The groundwater level decreased from 0.4 m to 0.8 m below the surface (i.e., the groundwater well went dry).

When comparing the observed minimum soil moistures at similar matric potentials of the different treatments, we can see that biochar amended treatments had generally higher minimum soil water contents by about 7% for Period I, 4% for Period II, and 2% for Period III (Figure 4). Using these soil water contents, assuming a soil column of 300 mm (15 cm around the soil moisture sensor) and an average evapotranspiration rate of 3.1 mm day^{-1}, the plants in biochar amended treatments would basically have 2 to 7 days of extra water to transpire.

4.2 | Impact of biochar on soil water retention curves

The soil water retention curves from the different treatments showed different shapes. Specifically, they had different volumetric water contents at a given soil matric potential and exhibited large within-treatment variability for θ from 5% to 10% (Figure 4). The soil water retention curves also shifted through time, ranging from close to field capacity to the wilting point with, those estimated for Period III covering the lower volumetric water contents relative to the other periods. The soil water retention curve of the BC1 treatment became more similar to the curves found in finer grained soils, which indicates increased water retention while the soil water retention curve for the BC2 treatment became more similar to the curves associated with coarser soils (based on the Genuchten parameters α and n, Table 1) indicating enhanced water flows. Generally, the biochar treatments showed an increased volumetric soil water content relative to the control treatment consistently across the ranges of observed soil matric potentials in all three periods (Figure 4, Table A2). The effect of biochar was quantified by the response ratios of the wilting point, field capacity and the van Genuchten parameters α and n. Most of these ratios were found to be larger than one (Table 1), which indicates increased soil water content for a given water potential value in the biochar amended treatments. Overall, the soil water retention curves of both biochar amended treatments showed a 7% (Period I) and 2% (Period III) higher soil water contents at similar matric potential relative to the control treatment, leading to more plant water available under similar conditions (Figure 4, Table 1) (Figure A1).

4.3 | Isotopic variability of rain, soil and groundwater

Overall, the $\delta^{18}O$ and d-excess of rainfall was between $-15.7‰$ and $-0.2‰$ ($S_D = 3.4‰$) and 0‰ and $+18‰$ ($S_D = 4.6‰$) respectively ($\delta^{18}O$ see Figure 5a, d-excess see Figure A2a and A3). The $\delta^{18}O$ and d-excess of the mobile soil water and groundwater collected on the different sampling days were between $-7.5‰$ and $-4.5‰$ ($S_D = 1.3‰$) and $-1.1‰$ and $+9.7‰$ ($S_D = 4.9‰$) respectively ($\delta^{18}O$ see Figure 5b–d d-excess see Figure A2b–d and A3). The within-treatment variability in isotopic composition of mobile soil water samples for each sample day was <1 ‰ for $\delta^{18}O$ and <6 ‰ for d-excess
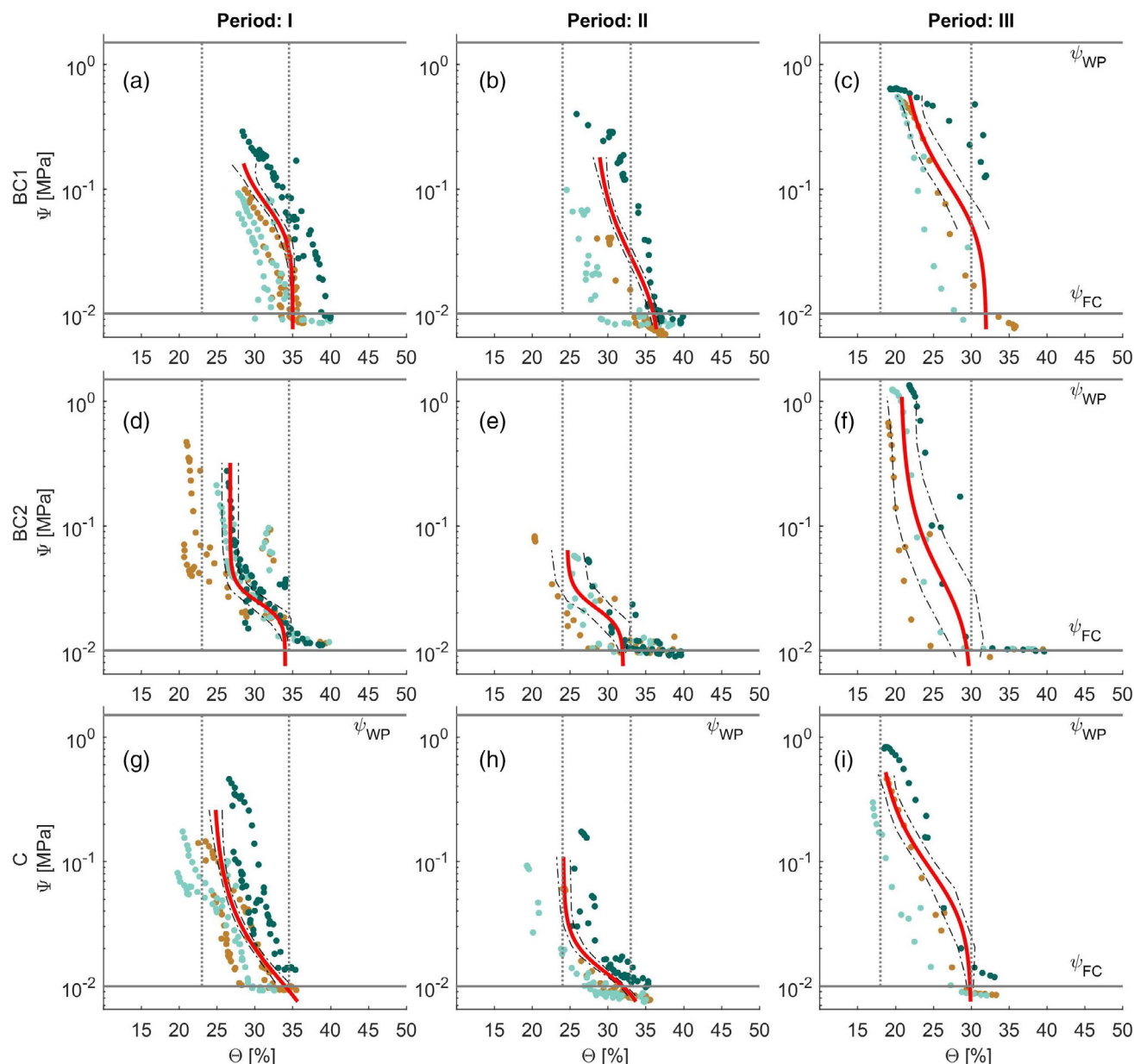
FIGURE 4 Soil matric potential as a function of average soil water content of the different plots (colours) for the treatments BC1 (a–c), BC2 (d–f) and C (g–i) and the periods I, II and III (columns). The fitted average soil water retention curves within a treatment using Equation (1) (red lines) including the 95% confidence interval (dot-dashed lines). The grey vertical lines indicate the minimum and maximum soil water content of the control treatment of that period.

(Figure 6). The $\delta^{18}O$ and *d-excess* of plant water were between $-8.7‰$ and $-2.7‰$ ($S_D = 3.7‰$) and $-14.6‰$ to $+3.2‰$ ($S_D = 11.4‰$) respectively ($\delta^{18}O$ see Figure 5b–d, *d-excess* see Figure A2b–d and A3). The within-treatment variability in isotopic composition of plant water samples on each sample day was >3 ‰ for $\delta^{18}O$ and >8 ‰ for *d-excess* (Figure 6). The within-treatment variability was smaller for the biochar amended treatments relative to the within-treatment variability in the control treatment (Figure 6).

During Period I, the isotopic composition of rainfall varied between $-5.6‰$ and $-0.2‰$ for $\delta^{18}O$ (Figure 5a) and from $-1.1‰$ to $+9‰$ for *d-excess* (Figure A2). On rainy days when rainfall

intensities were below 10 mm d^{-1}, sub-cloud evaporation may exert an important control on rainfall enrichment (Sánchez-Murillo et al., 2016, 2017) along with a potential for evaporated water in the sampler. For example, the observed fractionated isotopic compositions of these rain samples were often recorded to be <5‰ with regard to *d-excess*. The average isotopic composition of plant water in the different treatments decreased roughly from $+3.2‰$ to $-4‰$ for $\delta^{18}O$ and increased from roughly $-40‰$ to $+18‰$ for *d-excess* during Period I (Figures 5 and A2). In Period II, the isotopic composition of rainfall varied between $-3.7‰$ and $-12.7‰$ for $\delta^{18}O$ (Figure 5a) and $+6‰$ to $+11.8‰$ for *d-excess* (Figure A2). The average isotopic

TABLE 1 Response ratios (RR) for wilting point (θ_{WP}), minimum observed average volumetric soil water contents (θ_{min}) field capacity (θ_{FC}), and for the van Genuchten parameters α and n (Equation (1)) for BC1 and BC2. Parameters are derived for the average soil water retention curves of Figure 4 for periods I–III. A response ratio RR > 1 indicates that biochar has a positive effect on a soil water content while a RR $\approx$ 1 indicates that biochar has no effect, while RR < 1 indicates a negative response for the variable of interest

	BC	Period I	Period II	Period III
$\theta_{WP\ BC}\ \theta_{WP\ C}^{-1}$	1	1.36	1.46	1.18
	2	1.16	1.32	1.03
$\theta_{min\ BC}\ \theta_{min\ C}^{-1}$	1	1.12	1.16	1.17
	2	1.08	1.03	1.11
$\theta_{FC\ BC}\ \theta_{FC\ C}^{-1}$	1	1.08	1.14	1.04
	2	1.13	1.13	0.88
$\alpha_{BC}\ \alpha_C^{-1}$	1	1.29	0.50	0.68
	2	3.21	1.34	1.08
$n_{BC}\ n_C^{-1}$	1	1.00	0.89	1.47
	2	1.00	0.92	1.06

composition of plant water varied in all treatments between −7‰ and −2‰ for $\delta^{18}O$ and −11.8‰ to +9.2‰ for *d-excess*. It should be noted that there was a change from negative to positive *d-excess* for the plant water isotopic compositions between sampling days five and seven, indicating a change from highly fractionated isotopic compositions to compositions similar to that of rainfall. During the dry spell of Period III, no mobile soil water could be extracted from the suction lysimeters at 15 cm below the surface on sampling days 10 and 11. The average isotopic composition of xylem water varied between −7‰ to −6‰ for $\delta^{18}O$ and −7‰ to −2‰ for *d-excess*, showing a high fractionation signature (Figures 5, A2 and A3).

4.4 | Plant water in the dual isotope space

The rainfall isotopic compositions collected in our experiment fell along the GMWL and LMWL (Figure 7). The mobile soil water and groundwater isotopic samples from Period I were more fractionated compared to the mobile soil water isotopic samples from the wet Period II and III which fell more along the GMWL (Figure 8).
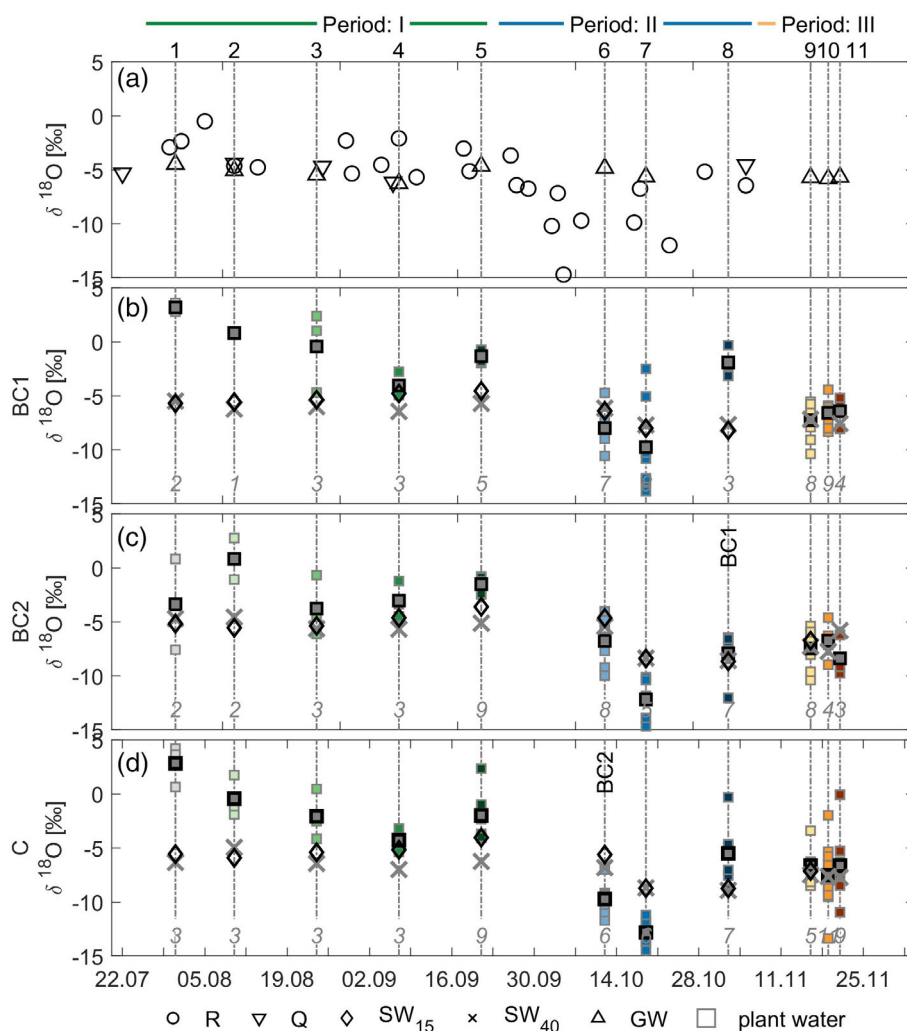

FIGURE 5 Time series of (a) $\delta^{18}O$ in rainfall (R), irrigation water (Q), groundwater (GW) and (b-d) average mobile soil water sampled at 15 cm (SW_{15}) and 40 cm (SW_{40}). The $\delta^{18}O$ of plant water (squares, where colours indicate the different sampling days) and its average (black square) are shown for the BC1 (b), BC2 (c) and control treatment (d), for sampling days 1–11 (indicated in each panel as vertical dashed lines and numbered on top of panel a). Period I, II and III are indicated on the top of panel a. italic numbers in panels b–d indicate the numbers of plants samples. Significant differences among the average plant water values (per treatment n > 3) of each sampling day are on the vertical dashed lines as letter of the treatment, for example, BC1, BC2 or C (Tukey's honestly significant difference criterion α = 0.05).
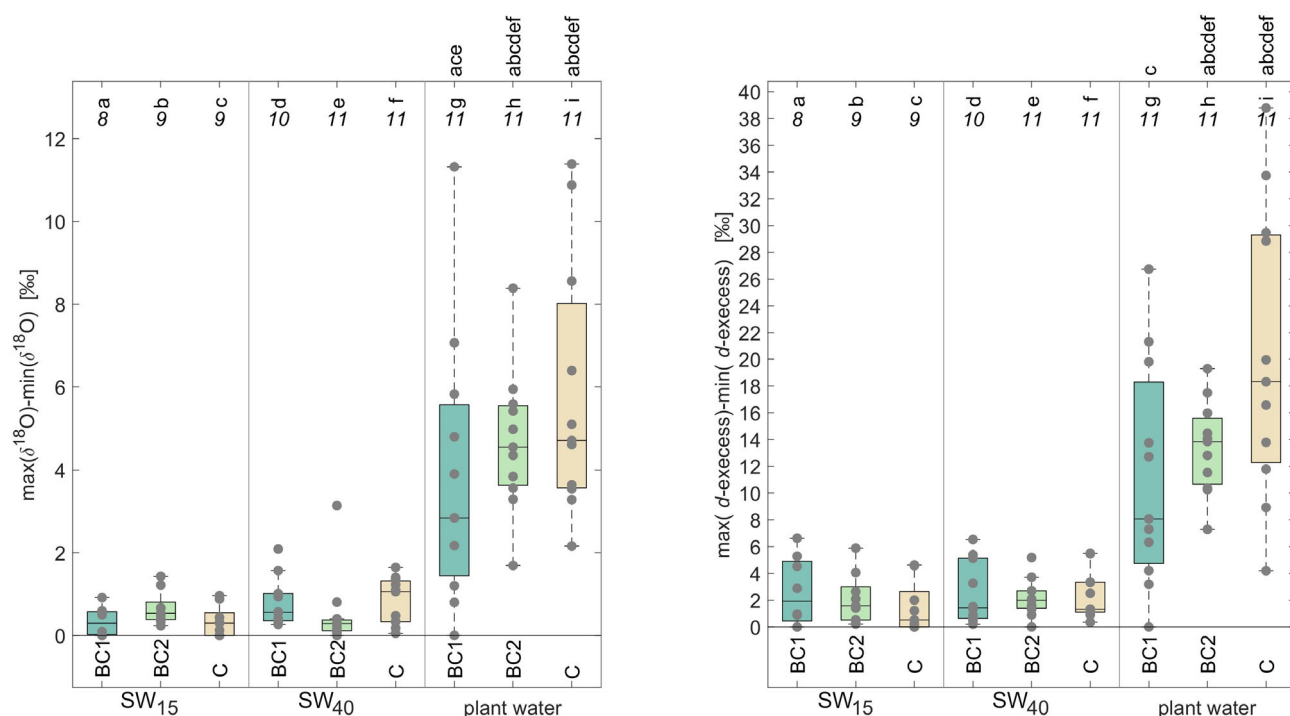
FIGURE 6 The variability in stable isotope composition $\delta^{18}O$ (left) and *d-excess* (right) expressed as range (maximum- minimum observed isotopic composition) for the mobile soil water collected at 15 cm (SW_{15}) and 40 cm (SW_{40}) below surface, and plant water in the BC1, BC2 and control treatment. The boxes show the range of values for different sample groups (showing the median and the interquartile range, with whiskers indicating 10th and 90th percentiles). Circles indicate the data points. Numbers above each box indicate the number of samples available. Letters on top of each box indicate significant differences among the average values of the different groups (Tukey's honestly significant difference criterion $\alpha = 0.05$).

The xylem water isotopic compositions from the different treatments and sampling periods were slightly but not significant different from each other in terms of $\delta^{18}O$ and δ^2H (Figures 6 and A3). Based on the difference in *d-excess* of xylem water and potential plant water sources e.g., rainfall, mobile soil water, and groundwater (Figure A3), one could interpret the plants consumed water from a pool of water that was not sampled in our experiment. However, the temporal lumped representation in boxplots (Figures 6 and A3) does not show the more detailed evolution of the stable isotope composition of xylem water which does follow a similar temporal evolution of the observed hydrometric variables (Figures 5 and 7). In Period I, the mobile soil- and groundwater were close to the GMWL while the xylem water samples from all treatments deviated from the GMWL. Since the xylem water signature had a strong evaporation signature in Period I and was different in their signature from the sampled mobile soil water, it is likely that plants consumed immobile soil water. In Period II, which was much wetter than Period I, the soil was replenished by rainfall and the mobile soil water acquired had the isotopic signature of rainfall. The xylem water samples were on or were close to the GMWL independent of the treatment and moved primarily along the GMWL. At the end of Period II, xylem water samples from BC1 and the control treatment showed a more fractioned signature and deviation from the GMWL compared to xylem water samples in BC2 treatment (Figure 7 b, e and h). During the dry Period III, all xylem

water samples deviated even more from the GMWL compared to in Period II and likely acquired the signature of residual rainfall that had fallen in Period II (Figure 7c,f,i).

5 | DISCUSSION

5.1 | Variable effect of biochar on the soil hydraulic properties

Incorporating two different types of biochar in plots planted with rice affected the soil hydraulic properties. In the BC1 treatment, amending biochar changed soil property to finer grained soils indicating increased water retention in respect of the control treatment a commonly expected impact of biochar additions (Fischer et al., 2018; Sun & Lu, 2014). Conversely, in the BC2 treatment, amending biochar enhanced water flows, which has been described as a potential impact of biochar additions (Fischer et al., 2018; Liu et al., 2017). Overall, the soil water retention curves of both biochar amended treatments showed a 7% (Period I) and 2% (Period III) higher soil water contents by which plants could translate into up to seven extra days of water available for the rice in the biochar plots relative to rice in non-treated soils.

The overall soil response to biochar amendments was comparable to the response found in other tropical soils (Obia et al., 2016). The
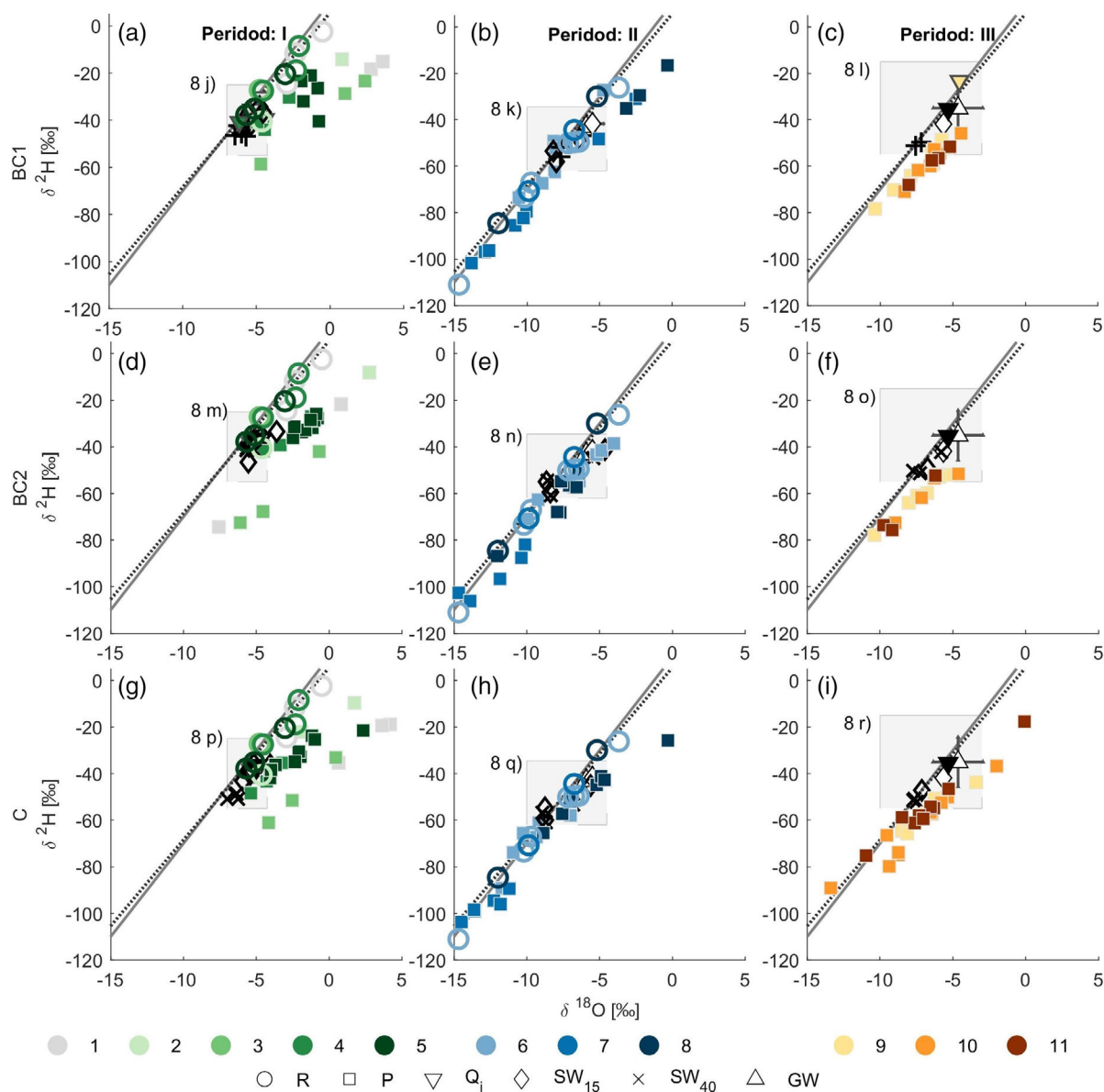
FIGURE 7 The dual isotope space with the isotopic composition of daily rainfall samples (circles), plant water samples (squares) for the treatments BC1 (a–c), BC2 (d–f) and C (g–i) and periods I–III (columns). Colours indicate the different sampling days. The local meteoric line (black dotted line) and global meteoric water line (grey solid line) are indicated in all panels. Isotopic compositions of irrigation, mobile soil water and groundwater vary within the grey shaded squares indicated as Figure 8j–r, and enlarged in Figure 8j–r.

soil water retention curves we found had a more irregular shape and a large within-treatment variability compared to laboratory derived curves reported in the literature (Iiyama, 2016; Morgan et al., 2001), which usually present one single continuous drying curve (e.g., Batool et al., 2015; Głąb et al., 2016 or Obia et al., 2016). Instead, the soil water retention curves in the present study were field derived and the result of temporally variable atmospheric forcing. Specifically, our observed within-treatment variability in the soil water retention curves was in the same order of magnitude as the responses due to differences in biochar application rates or due to differences in biochar typologies reported in laboratory studies (e.g., Batool et al., 2015; Głąb et al., 2016 or Obia et al., 2016).

Although the two biochar types tested were produced in different ways, their experimental application was similar (i.e., same application rate, similar particle size, application amount, depth, site characteristics and climate). One key distinction between the two biochar treatments was the application date, which may be important because aging can change the physical and chemical characteristics of biochar (Blanco-Canqui, 2017). Due to logistical constraints, biochar was introduced to the BC1 plot about 6 months before the BC2 plot. This allowed the biochar to age in situ and the disturbed soils to settle under the BC1 treatment. Thus, the BC2 soil likely had relatively larger macropores that could have increased the connectivity of the 20 cm soil layer where biochar was applied with deeper soil layers.
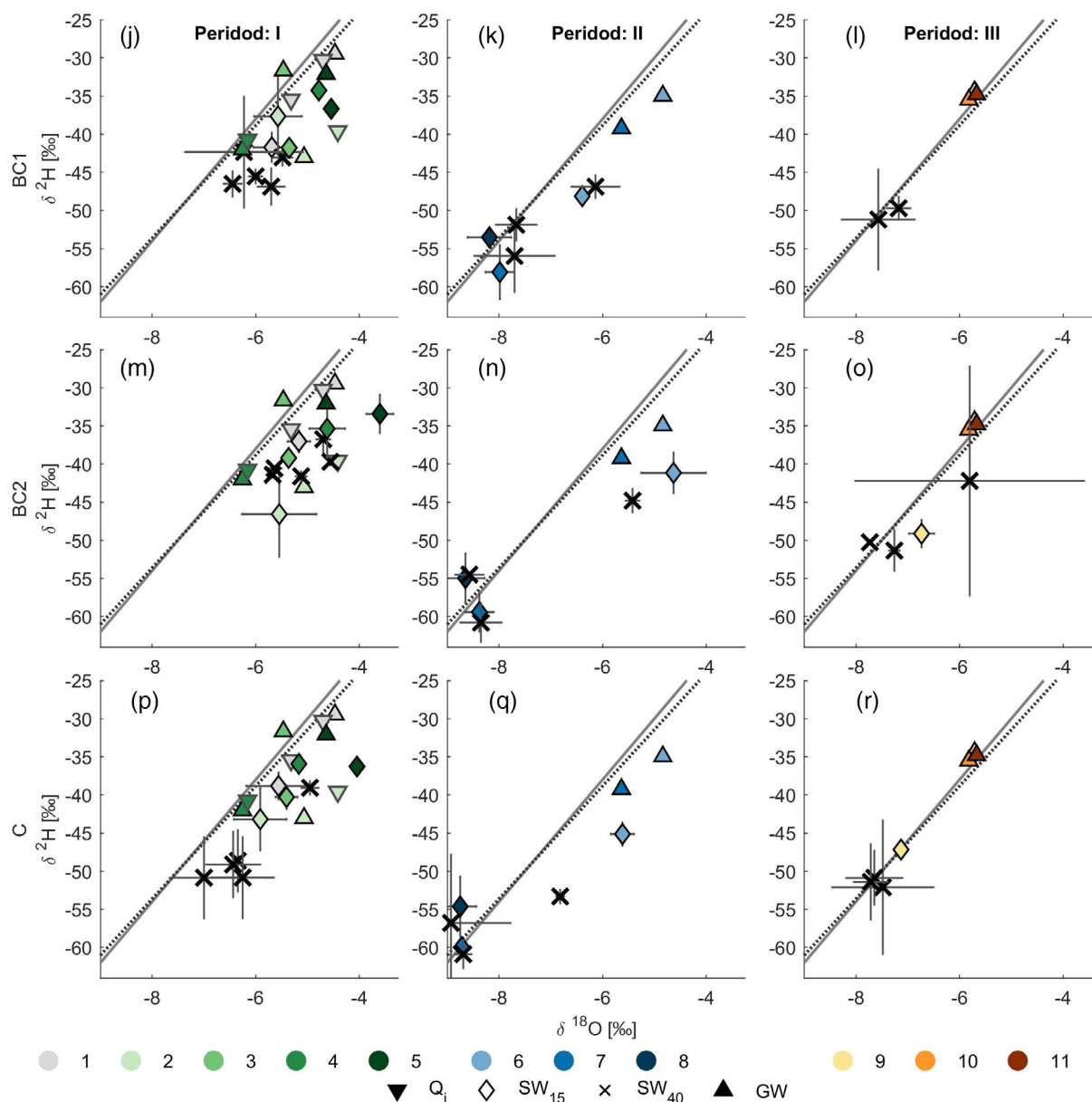
FIGURE 8 The dual isotope space with the isotopic composition of irrigation (down facing triangle), mobile soil water collected at 15 cm (SW$_{15}$, diamond) and 40 cm (SW$_{40}$, cross) and groundwater (upward facing triangle). The local meteoric line (black dotted line) and global meteoric water line (grey solid line) are indicated in all panels. The different treatments BC1 (j–l), BC2 (m–o) and C (p–r) and different periods I–III (columns) indicated in grey panels of Figure 7a–i. Colours indicate the different sampling days.

This difference in application timing relative to sampling may have influenced the hydraulic properties and created differences in the shape of the soil water retention curves in the two biochar treatments (Figure 4). Clearly, the interplay of all the possible biochar variables with all the possible site-specific heterogeneities makes it challenging to isolate the biochar effect in this experimental system and in agroecosystems in general. Taken altogether, these differences in biochar treatment responses and the relative impacts of both BC1 and BC2 treatments compared to the control plot highlight the potential for variability in biochar responses – which has been documented in the literature (Fischer et al., 2018) – creating ambiguity around predicting the response of biochar amendments at field scale. Although the

experimental design was somewhat unbalanced (different size of BC1 and C compared to BC2 and different biochar typology and age), which could be problematic when studying the effect of biochar on yield, the random and multiple plant sampling within each plot likely minimizes boundary effects or design effects relevant for our results. Instead, the suction lysimeters and soil moisture sensors considered in this study provide a similar and a rather small sampling or sensor footprint. While in-situ sensors provided useful insights on the temporal variably of different variables and differences within and between treatments, the informative value is spatially rather limited when compared with the remotely sensed spatial data presented by Jin et al. (2021). Therefore, future studies should combine spatial sparse but

high temporal in situ sensors with spatial snapshot multisensory information (hyperspectral and thermal imagery) obtained for example from unmanned aerial vehicles to estimate the gross primary productivity and water use efficiency allowing to investigate the effect of biochar at the field scale where management decisions are made (Jin et al., 2021).

5.2 | Stable isotopic composition of rice plant water

The isotopic data was useful to infer which pools of water the rice plants accessed. For example, the fractionation observed in the xylem water collected in the different treatments in Period I (Figure 7). indicates evaporative processes. A strong evaporation signal, i.e., a deviation of the isotopic composition of xylem water from the GMWL along an evaporation line, is in agreement with observations made in soil water of the top soil layer (Amin et al., 2020; Sprenger et al., 2016), in trees during the wet and dry season (Brooks et al., 2010) or in rice plants during different growing stages (Mahindawansha et al., 2018). This evaporation signal is also consistent with our high estimated evapotranspiration rates (average 3 mm day^{-1} up to 6 mm day^{-1}) which are typical for the Dry Corridor of Central America characterized by high solar radiation and air temperatures (Morillas et al., 2019). Hence, it is likely that during Period I, the young rice plants (root length rice <20 cm, e.g., Mahindawansha et al. (2018)) consumed the fractionated bulk soil water which was not sampled with the suction lysimeters at 15 cm below the surface.

From the initial strong evaporation signal observed in the xylem water during the drier Period I, the xylem water signatures changed to the proximity of GWML in the wet Period II. This indicates that the xylem water had a more temporal variable isotope composition compared to observations by Brooks et al. (2010) or Mahindawansha et al. (2018). Even in Period III, where it became increasingly difficult to extract water from suction lysimeters at 15 cm below the surface, the isotopic composition of xylem water deviated only minor from the GMWL. A change of the xylem water towards the GMWL could be because plants grew to their maximum heights during Period II. The plants with their now longer roots (root length rice >60 cm, e.g., Mahindawansha et al. (2018)) could reach deeper soil layers with more stable and older water stores, which was also observed in tall vegetation with deep roots (Allen et al., 2019; Amin et al., 2020). Since, biochar can increase the soil connectivity of shallow with deeper soil layers facilitating rainwater to infiltrate and reach deeper soil layers (Fischer et al., 2018), the rice plants could have consumed this deep soil water from rainfall. However, based on the isotopic compositions of mobile soil, groundwater in the biochar and control treatments were alike and rather temporal stable indicating there was a similar, i.e., no clear effect of biochar increasing the soil connectivity. Instead, the stable isotopic composition of xylem water was different from the mobile soil and groundwater but similar to the temporal isotopic composition of rainfall (Figures 5, 7, 8 and A2). This indicates

that the rice plants in the different treatments seem to have preferably consumed the temporally variable and isotopically labelled shallow and "newer" soil water from rainfall. Similar observations were made in natural ecosystems (e.g., van der Velde et al., 2015) and temperate grasslands (Bachmann et al., 2015) or rice paddies without biochar (Mahindawansha et al., 2018).

Since we were not able to extract bulk soil water for isotopic composition analysis, it was not possible to quantify plant water sources using two-end member or Bayesian mixing models (Layman et al., 2012; Rothfuss & Javaux, 2017). However, our isotopic data was useful to distinguish between rain, mobile soil water, and groundwater composition from the xylem water and deduce that rice plants grown in the biochar amended and control treatments access similar pools of water. Despite using the same sources of water, rice plants growing in biochar amended soils had access to more water (Figure 4) and thus could withstand longer dry spells. Still, even with this buffer of soil water storage, supplemental irrigation was required to facilitate plant growth during extended dry periods. Therefore, our results from one growing season demonstrate that biochar amendments can complement but not necessarily replace other water management strategies. Regardless of the potential advantages, as stated by Fischer et al. (2018) it must be noted that biochar as a water management tool does not adhere to a one size fits all approach but needs fine-tuning to climate, site, and plant characteristics to obtain stable and optimal yields.

6 | CONCLUSIONS

Amending soils with biochar is an emerging and promising practice improving the resilience of rainfed agriculture to climate variability by increasing the soil water and plant available water. In an experimental field study, consisting of two biochar treatments (differing in production, substrate and age of biochar but similar in application rate, particle size, application amount, depth, site characteristics and climate) and one control treatment, we observed that despite the differences the biochar amendments had generally 2% to 7% higher soil water content. As a result, plants in biochar amended treatments had more plant water relative to the control treatment. In addition, observed within-treatment variability in the soil water retention curves was in the same order of magnitude as one would expect from the literature describing responses due to different biochar application rates or different biochar typologies. Further, the isotopic composition of plant water in biochar and control treatments were rather similar indicating that rice plants in different treatments likely consumed similar water sources. Although it was not possible to quantify the water sources in detail, the stable isotope composition of plant water showed that the rice plants of the different treatments likely consumed soil water from antecedent rainfall. Despite the positive effects of biochar amendment to stabilize water supplies for the rice plants, additional water management strategies might be necessary for optimal plant growth and yield, for example, irrigation during extended dry periods.

CONFLICT OF INTEREST

The authors declare that they have no conflict of interest.

DATA AVAILABILITY STATEMENT

Upon acceptance, all of the research data that were required to create the plots will be available from the Bolin Center for Climate Research.

ORCID

Benjamin M. C. Fischer https://orcid.org/0000-0003-2530-6084
Laura Morillas https://orcid.org/0000-0002-5774-1366
Johanna Rojas Conejo https://orcid.org/0000-0002-9001-3694
Ricardo Sánchez-Murillo https://orcid.org/0000-0001-8721-8093
Andrea Suárez Serrano https://orcid.org/0000-0002-1930-3381
Jay Frentress https://orcid.org/0000-0003-3897-660X
Chih-Hsin Cheng https://orcid.org/0000-0001-5249-9817
Monica Garcia https://orcid.org/0000-0002-4587-8920
Stefano Manzoni https://orcid.org/0000-0002-5960-5712
Mark S. Johnson https://orcid.org/0000-0001-5070-7539
Steve W. Lyon https://orcid.org/0000-0002-1137-648X

REFERENCES

Agegnehu, G., Srivastava, A. K., & Bird, M. I. (2017). The role of biochar and biochar-compost in improving soil quality and crop performance: A review. *Applied Soil Ecology*, 119, 156–170. https://doi.org/10.1016/j.apsoil.2017.06.008

Allen, R. G., Pereira, L. S., Raes, D., & Smith, M. (1998). *Crop evapotranspiration-guidelines for computing crop water requirements* (p. 56). FAO.

Allen, S. T., Kirchner, J. W., Braun, S., Siegwolf, R. T. W., & Goldsmith, G. R. (2019). Seasonal origins of soil water used by trees. *Hydrology and Earth System Sciences*, 23(2), 1199–1210. https://doi.org/10.5194/hess-23-1199-2019

Amin, A., Zuecco, G., Geris, J., Schwendenmann, L., McDonnell, J. J., Borga, M., & Penna, D. (2020). Depth distribution of soil water sourced by plants at the global scale: A new direct inference approach. *Ecohydrology*, 13(2), e2177. https://doi.org/10.1002/eco.2177

Bachmann, D., Gockele, A., Ravenek, J. M., Roscher, C., Strecker, T., Weigelt, A., & Buchmann, N. (2015). No evidence of complementary water use along a plant species richness gradient in temperate experimental grasslands. *PLoS One*, 10(1), 1–14. https://doi.org/10.1371/journal.pone.0116367

Batool, A., Taj, S., Rashid, A., Khalid, A., Qadeer, S., Saleem, A. R., & Ghufran, M. A. (2015). Potential of soil amendments (biochar and gypsum) in increasing water use efficiency of Abelmoschus esculentus L. Moench. *Frontiers in Plant Science*, 6(September), 1–13. https://doi.org/10.3389/fpls.2015.00733

Benettin, P., Volkmann, T. H. M., von Freyberg, J., Frentress, J., Penna, D., Dawson, T. E., & Kirchner, J. W. (2018). Effects of climatic seasonality on the isotopic composition of evaporating soil waters. *Hydrology and Earth System Sciences*, 22(5), 2881–2890. https://doi.org/10.5194/hess-22-2881-2018

Biazin, B., Sterk, G., Temesgen, M., Abdulkedir, A., & Stroosnijder, L. (2012). Rainwater harvesting and management in rainfed agricultural systems in sub-Saharan Africa – A review. *Physics and Chemistry of the Earth, Parts A/B/C*, 47–48, 139–151. https://doi.org/10.1016/j.pce.2011.08.015

Birkel C, Brenes A, Sánchez-Murillo R. 2017. The Tempisque-Bebedero catchment system: Energy-water-food consensus in the seasonally dry tropics of northwestern Costa Rica. In Nexus outlook: Assessing Resource Use Challenges in the Water, Energy and Food NexusTH-Koeln, University of Applied Sciences. https://www.water-energy-food.org/fileadmin/user_upload/files/documents/others/Outlook-Nexus_Assessing_Resource_Use_Challenges.pdf

Blanco-Canqui, H. (2017). Biochar and soil physical properties. *Soil Science Society of America Journal*, 81(4), 687–711. https://doi.org/10.2136/sssaj2017.01.0017

Brooks, R. J., Barnard, H. R., Coulombe, R., & McDonnell, J. J. (2010). Eco-hydrologic separation of water between trees and streams in a Mediterranean climate. *Nature Geoscience*, 3(2), 100–104. https://doi.org/10.1038/ngeo722

Castelli, G., Bresci, E., Castelli, F., Hagos, E. Y., & Mehari, A. (2018). A participatory design approach for modernization of spate irrigation systems. *Agricultural Water Management*, 210, 286–295. https://doi.org/10.1016/j.agwat.2018.08.030

Craig, H. (1961). Isotopic variations in meteoric waters. *Science*, 133(3465), 1702–1703. https://doi.org/10.1126/science.133.3465.1702

Dansgaard, W. (1964). Stable isotopes in precipitation. *Tellus*, 16(4), 436–468. https://doi.org/10.1111/j.2153-3490.1964.tb00181.x

Dawson, T. E., & Ehleringer, J. R. (1991). Streamside trees that do not use stream water. *Nature*, 350(6316), 335–337. https://doi.org/10.1038/350335a0

de Fraiture, C., Karlberg, L., & Rockström, J. (2009). Can rainfed agriculture feed the world? An assessment of potentials and risk. In *Rainfed agriculture: Unlocking the potential* (pp. 124–132). CAB International.

de Fraiture, C., & Wichelns, D. (2010). Satisfying future water demands for agriculture. *Agricultural Water Management*, 97(4), 502–511. https://doi.org/10.1016/j.agwat.2009.08.008

Diogenes Cubero F, Maria José Elizondo A. 2014. Estudio detallado de suelos y capacidad de uso de las tierras de estación experimental enrique jiménez núñez (detailed study of soils and capacity of use of the lands of experimental station enrique jiménez núñez). Instituto Nacional de Innovación y Transferencia en Tecnología Agropecuaria, Cañas.

Enfors, E. I. I., & Gordon, L. J. J. (2007). Analysing resilience in dryland agro-ecosystems: A case study of the Makanya catchment in Tanzania

over the past 50 years. *Land Degradation & Development*, *18*(6), 680–696. https://doi.org/10.1002/ldr.807

Falkenmark, M. (1997). Society's interaction with the water cycle: A conceptual framework for a more holistic approach. *Hydrological Sciences Journal*, *42*(4), 451–466. https://doi.org/10.1080/02626669709492046

Famiglietti, J. S. (2014). The global groundwater crisis. *Nature Climate Change*, *4*(11), 945–948. https://doi.org/10.1038/nclimate2425

Feng, X., Porporato, A., & Rodriguez-Iturbe, I. (2013). Changes in rainfall seasonality in the tropics. *Nature Climate Change*, *3*(9), 811–815. https://doi.org/10.1038/nclimate1907

Fischer, B. M. C., Manzoni, S., Morillas, L., Garcia, M., Johnson, M. S., & Lyon, S. W. (2018). Improving agricultural water use efficiency with biochar – A synthesis of biochar effects on water storage and fluxes across scales. *Science of the Total Environment*, *657*, 853–862. https://doi.org/10.1016/j.scitotenv.2018.11.312

Fischer, B. M. C., Mul, M. L., & Savenije, H. H. G. (2013). Determining spatial variability of dry spells: A Markov-based method, applied to the Makanya catchment. *Tanzania. Hydrology and Earth System Sciences*, *17*(6), 2161–2170. https://doi.org/10.5194/hess-17-2161-2013

Fischer, B. M. C., Stähli, M., & Seibert, J. (2017). Pre-event water contributions to runoff events of different magnitude in pre-alpine headwaters. *Hydrology Research*, *48*(1), 28–47. https://doi.org/10.2166/nh.2016.176

Giorgi, F. (2006). Climate change hot-spots. *Geophysical Research Letters*, *33*(8), L08707. https://doi.org/10.1029/2006GL025734

Głąb, T., Palmowska, J., Zaleski, T., & Gondek, K. (2016). Effect of biochar application on soil hydrological properties and physical quality of sandy soil. *Geoderma*, *281*, 11–20. https://doi.org/10.1016/j.geoderma.2016.06.028

Gonfiantini, R. (1986). Chapter 3 - Environmental isotopes in lake studies. In P. Fritz & J. C. Fontes (Eds.), *The terrestrial environment, B* (pp. 113–168). Elsevier. https://doi.org/10.1016/B978-0-444-42225-5.50008-5

Hidalgo, H. G., Alfaro, E. J., Amador, J. A., & Bastidas, Á. (2019). Precursors of quasi-decadal dry-spells in the Central America dry corridor. *Climate Dynamics*, *53*(3), 1307–1322. https://doi.org/10.1007/s00382-019-04638-y

IAEA. 2009. Reference sheet for VSMOW2 and SLAP2 international measurement standards. Issued 200902-13.

Iiyama, I. (2016). Differences between field-monitored and laboratory-measured soil moisture characteristics. *Soil Science and Plant Nutrition*, *62*(5–6), 416–422. https://doi.org/10.1080/00380768.2016.1242367

Imbach, P., Chou, S. C., Lyra, A., Rodrigues, D., Rodriguez, D., Latinovic, D., Siqueira, G., Silva, A., Garofolo, L., & Georgiou, S. (2018). Future climate change scenarios in Central America at high spatial resolution. *PLoS One*, *13*(4), e0193570. https://doi.org/10.1371/journal.pone.0193570

Jasechko, S., Perrone, D., Befus, K. M., Bayani Cardenas, M., Ferguson, G., Gleeson, T., Luijendijk, E., McDonnell, J. J., Taylor, R. G., Wada, Y., et al. (2017). Global aquifers dominated by fossil groundwaters but wells vulnerable to modern contamination. *Nature Geoscience*, *10*(6), 425–429. https://doi.org/10.1038/ngeo2943

Jeffery, S., Abalos, D., Prodana, M., Bastos, A. C., Van Groenigen, J. W., Hungate, B. A., & Verheijen, F. (2017). Biochar boosts tropical but not temperate crop yields. *Environmental Research Letters*, *12*(5), 1748–9326. https://doi.org/10.1088/1748-9326/aa67bd

Jeffery, S., Meinders, M. B. J., Stoof, C. R., Bezemer, T. M., van de Voorde, T. F. J., Mommer, L., & van Groenigen, J. W. (2015). Biochar application does not improve the soil hydrological function of a sandy soil. *Geoderma*, *251–252*, 47–54. https://doi.org/10.1016/j.geoderma.2015.03.022

Jin, H., Köppl, C. J., Fischer, B. M. C., Rojas-Conejo, J., Johnson, M. S., Morillas, L., Lyon, S. W., Durán-Quesada, A. M., Suárez-Serrano, A., Manzoni, S., & Garcia, M. (2021). Drone-based hyperspectral and thermal imagery for quantifying upland rice productivity and water use efficiency after biochar application. *Remote Sensing*, *13*(10), 1866. https://doi.org/10.3390/rs13101866

Kätterer, T., Roobroeck, D., Andrén, O., Kimutai, G., Karltun, E., Kirchmann, H., Nyberg, G., Vanlauwe, B., & Röing de Nowina, K. (2019). Biochar addition persistently increased soil fertility and yields in maize-soybean rotations over 10 years in sub-humid regions of Kenya. *Field Crops Research*, *235*, 18–26. https://doi.org/10.1016/j.fcr.2019.02.015

Klaus, J., & McDonnell, J. J. (2013). Hydrograph separation using stable isotopes: Review and evaluation. *Journal of Hydrology*, *505*, 47–64. https://doi.org/10.1016/j.jhydrol.2013.09.006

Knutson, T. R., Delworth, T. L., Dixon, K. W., Held, I. M., Lu, J., Ramaswamy, V., Schwarzkopf, M. D., Stenchikov, G., & Stouffer, R. J. (2006). Assessment of twentieth-century regional surface temperature trends using the GFDL CM2 coupled models. *Journal of Climate*, *19*(9), 1624–1651. https://doi.org/10.1175/JCLI3709.1

Koeniger, P., Gaj, M., Beyer, M., & Himmelsbach, T. (2016). Review on soil water isotope-based groundwater recharge estimations. *Hydrological Processes*, *30*(16), 2817–2834. https://doi.org/10.1002/hyp.10775

Koeniger, P., Marshall, J. D., Link, T., & Mulch, A. (2011). An inexpensive, fast, and reliable method for vacuum extraction of soil and plant water for stable isotope analyses by mass spectrometry. *Rapid Communications in Mass Spectrometry*, *25*(20), 3041–3048. https://doi.org/10.1002/rcm.5198

Layman, C. A., Araujo, M. S., Boucek, R., Hammerschlag-Peyer, C. M., Harrison, E., Jud, Z. R., Matich, P., Rosenblatt, A. E., Vaudo, J. J., Yeager, L. A., Post, D. M., & Bearhop, S. (2012). Applying stable isotopes to examine food-web structure: An overview of analytical tools. *Biological Reviews*, *87*(3), 545–562. https://doi.org/10.1111/j.1469-185X.2011.00208.x

Lim, T.-J., & Spokas, K. (2018). Impact of biochar particle shape and size on saturated hydraulic properties of soil. *Korean Journal of Environmental Agriculture*, *37*(1), 1–8.

Liu, C., Wang, H., Tang, X., Guan, Z., Reid, B. J., Rajapaksha, A. U., Ok, Y. S., & Sun, H. (2016). Biochar increased water holding capacity but accelerated organic carbon leaching from a sloping farmland soil in China. *Environmental Science and Pollution Research*, *23*(2), 995–1006. https://doi.org/10.1007/s11356-015-4885-9

Liu, Z., Dugan, B., Masiello, C. A., & Gonnermann, H. M. (2017). Biochar particle size, shape, and porosity act together to influence soil water properties. *PLoS One*, *12*(6), 1–19. https://doi.org/10.1371/journal.pone.0179079

Lyon, S. W., Fischer, B. M. C., Morillas, L., Rojas Conejo, J., Sánchez-Murillo, R., Suárez Serrano, A., Frentress, J., Cheng, C.-H., Garcia, M., & Johnson, M. S. (2022). On the potential of biochar soil amendments as a sustainable water management strategy. *Sustainability*, *14*(12), 7026. https://doi.org/10.3390/su14127026

Magaña, V., Amador, J. A., & Medina, S. (1999). The midsummer drought over Mexico and Central America. *Journal of Climate, 12*(6), 1577–1588. https://doi.org/10.1175/1520-0442(1999)012<1577:TMDOMA>2.0.CO;2

Mahindawansha, A., Orlowski, N., Kraft, P., Rothfuss, Y., Racela, H., & Breuer, L. (2018). Quantification of plant water uptake by water stable isotopes in rice paddy systems. *Plant and Soil*, *429*(1), 281–302. https://doi.org/10.1007/s11104-018-3693-7

Makurira, H., Mul, M. L., Vyagusa, N. F., Uhlenbrook, S., & Savenije, H. H. G. (2007). Evaluation of community-driven smallholder irrigation in dryland south Pare Mountains, Tanzania: A case study of Manoo micro dam. *Physics and Chemistry of the Earth, Parts A/B/C*, *32*(15–18), 1090–1097. https://doi.org/10.1016/j.pce.2007.07.020

McDonnell, J. J. (2014). The two water worlds hypothesis: Ecohydrological separation of water between streams and trees? *WIREs Water*, *1*(4), 323–329. https://doi.org/10.1002/wat2.1027

Morgan, K. T., Parsons, L. R., & Adair, W. T. (2001). Comparison of laboratory- and field-derived soil water retention curves for a fine sand soil using tensiometric, resistance and capacitance methods. *Plant and Soil*, *234*(2), 153–157. https://doi.org/10.1023/A:1017915114685

Morillas, L., Hund, S. V., & Johnson, M. S. (2019). Water use dynamics in double cropping of Rainfed upland Rice and irrigated melons produced

under drought-prone tropical conditions. *Water Resources Research*, 55(5), 4110–4127. https://doi.org/10.1029/2018WR023757

Muñoz-Villers, L. E., Geris, J., Alvarado-Barrientos, M. S., Holwerda, F., & Dawson, T. (2020). Coffee and shade trees show complementary use of soil water in a traditional agroforestry ecosystem. *Hydrology and Earth System Sciences*, 24(4), 1649–1668. https://doi.org/10.5194/hess-24-1649-2020

Mutiro, J., Makurira, H., Senzanje, A., & Mul, M. L. (2006). Water productivity analysis for smallholder rainfed systems: A case study of Makanya catchment, Tanzania. *Physics and Chemistry of the Earth, Parts A/B/C*, 31(15–16), 901–909. https://doi.org/10.1016/j.pce.2006.08.019

Narseh Kumar, M., Murthy, C. S., Sesha Sai, M. V. R., & Roy, P. S. (2009). On the use of standardized precipitation index (SPI) for drought intensity assessment. *Meteorological Applications*, 16(3), 381–389. https://doi.org/10.1002/met.136

Nelissen, V., Ruysschaert, G., Manka Abusi, D., D' Hose, T., De Beuf, K., Al-Barri, B., Cornelis, W., & Boeckx, P. (2015). Impact of a woody biochar on properties of a sandy loam soil and spring barley during a two-year field experiment. *European Journal of Agronomy*, 62, 65–78. https://doi.org/10.1016/j.eja.2014.09.006

Novak, J., Ro, K., Ok, Y. S., Sigua, G., Spokas, K., Uchimiya, S., & Bolan, N. (2016). Biochars multifunctional role as a novel technology in the agricultural, environmental, and industrial sectors. *Chemosphere*, 142, 1–3. https://doi.org/10.1016/j.chemosphere.2015.06.066

Obia, A., Mulder, J., Martinsen, V., Cornelissen, G., & Børresen, T. (2016). In situ effects of biochar on aggregation, water retention and porosity in light-textured tropical soils. *Soil and Tillage Research*, 155, 35–44. https://doi.org/10.1016/j.still.2015.08.002

Omondi, M. O., Xia, X., Nahayo, A., Liu, X., Korai, P. K., & Pan, G. (2016). Quantification of biochar effects on soil hydrological properties using meta-analysis of literature data. *Geoderma*, 274, 28–34. https://doi.org/10.1016/j.geoderma.2016.03.029

Oppong Danso, E., Yakubu, A., Kugblenu Darrah, Y. O., Arthur, E., Manevski, K., Sabi, E. B., Abenney-Mickson, S., Ofori, K., Plauborg, F., & Andersen, M. N. (2019). Impact of rice straw biochar and irrigation on maize yield, intercepted radiation and water productivity in a tropical sandy clay loam. *Field Crops Research*, 243, 107628. https://doi.org/10.1016/j.fcr.2019.107628

Penna, D., Geris, J., Hopp, L., & Scandellari, F. (2020). Water sources for root water uptake: Using stable isotopes of hydrogen and oxygen as a research tool in agricultural and agroforestry systems. *Agriculture, Ecosystems & Environment*, 291, 106790. https://doi.org/10.1016/j.agee.2019.106790

Penna, D., Hopp, L., Scandellari, F., Allen, S. T., Benettin, P., Beyer, M., Geris, J., Klaus, J., Marshall, J. D., Schwendenmann, L., Volkmann, T. H. M., von Freyberg, J., Amin, A., Ceperley, N., Engel, M., Frentress, J., Giambastiani, Y., McDonnell, J. J., Zuecco, G., … Kirchner, J. W. (2018). Ideas and perspectives: Tracing terrestrial ecosystem water fluxes using hydrogen and oxygen stable isotopes – Challenges and opportunities from an interdisciplinary perspective. *Biogeosciences*, 15(21), 6399–6415. https://doi.org/10.5194/bg-15-6399-2018

Prechsl, U. E., Gilgen, A. K., Kahmen, A., & Buchmann, N. (2014). Reliability and quality of water isotope data collected with a low-budget rain collector. *Rapid Communications in Mass Spectrometry*, 28(8), 879–885. https://doi.org/10.1002/rcm.6852

Reyes-Cabrera, J., Erickson, J. E., Leon, R. G., Silveira, M. L., Rowland, D. L., Sollenberger, L. E., & Morgan, K. T. (2017). Converting bahiagrass pasture land to elephantgrass bioenergy production enhances biomass yield and water quality. *Agriculture, Ecosystems and Environment*, 248(July), 20–28. https://doi.org/10.1016/j.agee.2017.07.021

Rockström, J. (1999). On-farm green water estimates as a tool for increased food production in water scarce regions. *Physics and Chemistry of the Earth, Part B: Hydrology, Oceans and Atmosphere*, 24(4), 375–383. https://doi.org/10.1016/S1464-1909(99)00016-7

Rothfuss, Y., & Javaux, M. (2017). Reviews and syntheses: Isotopic approaches to quantify root water uptake: A review and comparison of methods. *Biogeosciences*, 14(8), 2199–2224. https://doi.org/10.5194/bg-14-2199-2017

Sánchez-Murillo, R., & Birkel, C. (2016). Groundwater recharge mechanisms inferred from isoscapes in a complex tropical mountainous region. *Geophysical Research Letters*, 43(10), 5060–5069. https://doi.org/10.1002/2016GL068888

Sánchez-Murillo, R., Birkel, C., Welsh, K., Esquivel-Hernández, G., Corrales-Salazar, J., Boll, J., Brooks, E., Roupsard, O., Sáenz-Rosales, O., Katchan, I., Arce-Mesén, R., Soulsby, C., & Araguás-Araguás, L. J. (2016). Key drivers controlling stable isotope variations in daily precipitation of Costa Rica: Caribbean Sea versus eastern Pacific Ocean moisture sources. *Water Isotope Systematics*, 131, 250–261. https://doi.org/10.1016/j.quascirev.2015.08.028

Sánchez-Murillo, R., Durán-Quesada, A. M., Birkel, C., Esquivel-Hernández, G., & Boll, J. (2017). Tropical precipitation anomalies and d-excess evolution during El Niño 2014-16. *Hydrological Processes*, 31(4), 956–967. https://doi.org/10.1002/hyp.11088

Sánchez-Murillo, R., Esquivel-Hernández, G., Birkel, C., Correa, A., Welsh, K., Durán-Quesada, A. M., Sánchez-Gutiérrez, R., & Poca, M. (2020). Tracing water sources and fluxes in a dynamic tropical environment: From observations to modeling. *Frontiers in Earth Science*, 8, 438. https://doi.org/10.3389/feart.2020.571477

Sánchez-Murillo, R., Esquivel-Hernández, G., Corrales-Salazar, J. L., Castro-Chacón, L., Durán-Quesada, A. M., Guerrero-Hernández, M., Delgado, V., Barberena, J., Montenegro-Rayo, K., Calderón, H., Chevez, C., Peña-Paz, T., García-Santos, S., Ortiz-Roque, P., Alvarado-Callejas, Y., Benegas, L., Hernández-Antonio, A., Matamoros-Ortega, M., Ortega, L., & Terzer-Wassmuth, S. (2020). Tracer hydrology of the data-scarce and heterogeneous central American isthmus. *Hydrological Processes*, 34(11), 2660–2675. https://doi.org/10.1002/hyp.13758

Saxena R. 1987. Oxygen-18 fractionation in nature and estimation of groundwater recharge [Rayleigh distillation formula, reverse Rayleigh process, throughfall]. Report-University of Uppsala, Department of Physical Geography, Hydrological Division Series A (Sweden).

Sheng, Y., & Zhu, L. (2018). Biochar alters microbial community and carbon sequestration potential across different soil pH. *Science of the Total Environment*, 622–623, 1391–1399. https://doi.org/10.1016/j.scitotenv.2017.11.337

Sprenger, M., Leistert, H., Gimbel, K., & Weiler, M. (2016). Illuminating hydrological processes at the soil-vegetation-atmosphere interface with water stable isotopes. *Reviews of Geophysics*, 54(3), 674–704. https://doi.org/10.1002/2015RG000515

Stumpp, C., Maloszewski, P., Stichler, W., & Fank, J. (2009). Environmental isotope (δ18O) and hydrological data to assess water flow in unsaturated soils planted with different crops: Case study lysimeter station "Wagna" (Austria). *Journal of Hydrology*, 369(1), 198–208. https://doi.org/10.1016/j.jhydrol.2009.02.047

Sun, F., & Lu, S. (2014). Biochars improve aggregate stability, water retention, and pore-space properties of clayey soil. *Journal of Plant Nutrition and Soil Science*, 177(1), 26–33. https://doi.org/10.1002/jpln.201200639

Sundberg, C., Karltun, E., Gitau, J. K., Kätterer, T., Kimutai, G. M., Mahmoud, Y., Njenga, M., Nyberg, G., Roing de Nowina, K., Roobroeck, D., & Sieber, P. (2020). Biochar from cookstoves reduces greenhouse gas emissions from smallholder farms in Africa. *Mitigation and Adaptation Strategies for Global Change*, 25, 953–967. https://doi.org/10.1007/s11027-020-09920-7

van der Velde, Y., Heidbüchel, I., Lyon, S. W., Nyberg, L., Rodhe, A., Bishop, K., & Troch, P. A. (2015). Consequences of mixing assumptions for time-variable travel time distributions: Mixing assumptions and time-variable travel time distributions. *Hydrological Processes*, 29(16), 3460–3474. https://doi.org/10.1002/hyp.10372

Van Genuchten, M. T. (1980). A closed-form equation for predicting the hydraulic conductivity of unsaturated soils. *Soil Science Society of America Journal*, *44*(5), 892–898.

Vico, G., & Brunsell, N. A. (2018). Tradeoffs between water requirements and yield stability in annual vs. perennial crops. *Advances in Water Resources*, *112*, 189–202. https://doi.org/10.1016/j.advwatres.2017.12.014

Vico, G., & Porporato, A. (2015). Ecohydrology of agroecosystems: Quantitative approaches towards sustainable irrigation. *Bulletin of Mathematical Biology*, *77*(2), 298–318. https://doi.org/10.1007/s11538-014-9988-9

Zhang, D., Yan, M., Niu, Y., Liu, X., van Zwieten, L., Chen, D., Bian, R., Cheng, K., Li, L., Joseph, S., Zheng, J., Zhang, X., Zheng, J., Crowley, D., Filley, T. R., & Pan, G. (2016). Is current biochar research addressing global soil constraints for sustainable agriculture? *Agriculture, Ecosystems & Environment*, *226*, 25–32. https://doi.org/10.1016/j.agee.2016.04.010

SUPPORTING INFORMATION

Additional supporting information can be found online in the Supporting Information section at the end of this article.

APPENDIX A

TABLE A1 Soil characteristics of the experimental site

	BC1	BC2	C
Soil (0–20 cm) texture sand/silt/clay	34/30/36		
Infiltration capacity wet/dry season (mm h^{-1})	15/30	15/40	8/40
pH	6.5	6.3	6.4
Ca (mol kg-1)	11.77	12.43	11.77
Mg (mol kg^{-1})	2.60	2.63	2.47
K (mol kg^{-1})	0.87	0.97	0.80
P (mg L^{-1})	22.3	29.0	21.6
Zn (mg L^{-1})	3.2	3.3	3.1
Mn (mg L^{-1})	24.0	30.6	22.0
Cu (mg L^{-1})	9.3	11.0	9.6
Fe (mg L^{-1})	43.00	57.33	45.00
Organic C (%)	2.29	2.18	2.16
Total N (%)	0.15		

TABLE A2 The fitted parameters θ_r, α and n the average soil water retention curves of the different treatments (BC1, BC2 and C) and the periods I–III of Equation 1 with the 95% confidence interval in brackets

	BC1			BC2			C		
	Period			Period			Period		
	I	II	III	I	II	III	I	II	III
θ_r	0.2 (−0.2, 0.6)	0.3 (0.3, 0.3)	0.2 (0.2, 0.2)	0.3 (0.3, 0.3)	0.3 (0.2, 0.3)	0.2 (0.2, 0.2)	0.2 (0.2, 0.3)	0.3 (0.2, 0.3)	0.2 (0.2, 0.2)
α	13 (−6.7, 33)	78 (65, 90)	18 (8.1, 29)	44 (36, 52)	49 (29, 70)	34 (−14, 81)	27 (20, 34)	75 (61, 88)	58 (30, 85)
n	2.5 (−0.3, 5.4)	2.6 (1.8, 3.4)	2 (0.9, 3.1)	5.7 (1.4, 10)	5.1 (−0.2, 12)	2 (0.2, 3.8)	3 (1.2, 4.8)	10 (−0.4, 24)	2 (1.2, 2.9)

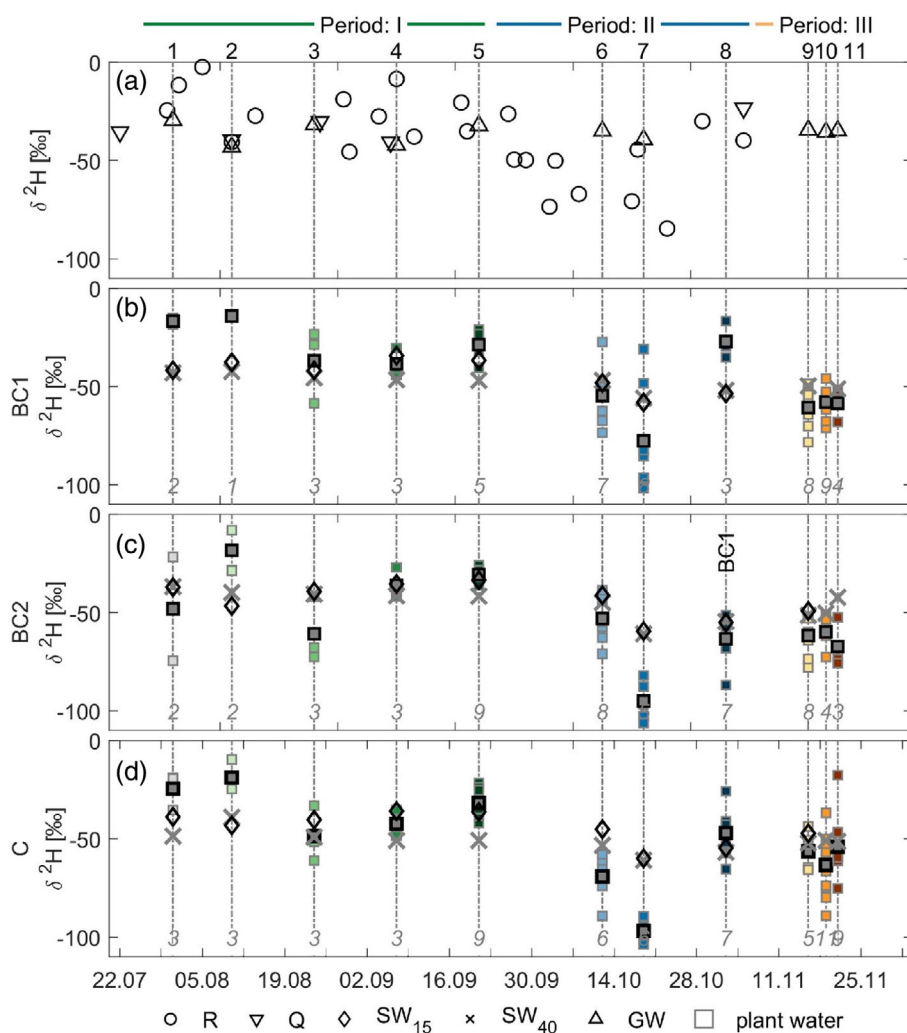**FIGURE A1** Time series of (a) δ^2H in rainfall (R), irrigation water (Q), groundwater (GW) and (b–d) average mobile soil water sampled at 15 cm (SW$_{15}$) and 40 cm (SW$_{40}$). The δ^2H of plant water (squares, where colours indicate the different sampling days) and its average (black square) are shown for the BC1 (b), BC2 (c) and control treatment (d), for sampling days 1–11 (indicated in each panel as vertical dashed lines and numbered on top of panel a). Period I, II and III are indicated on the top of panel a. italic numbers in panels b–d indicate the numbers of plants samples. Significant differences among the average plant water values (per treatment $n > 3$) of each sampling day are on the vertical dashed lines as letter of the treatment, for example, BC1, BC2 or C (Tukey's honestly significant difference criterion $\alpha = 0.05$).

FIGURE A2 Time series of (a) d-excess in rainfall (R), irrigation water (Q), groundwater (GW) and (b–d) average mobile soil water sampled at 15 cm (SW$_{15}$) and 40 cm (SW$_{40}$). The *d-excess* of plant water (squares, where colours indicate the different sampling days) and its average (black square) are shown for the BC1 (b), BC2 (c) and control treatment (d), for sampling days 1–11 (indicated in each panel as vertical dashed lines and numbered on top of panel a). Period I, II and III are indicated on the top of panel a. italic numbers in panels b–d indicate the numbers of plants samples. Significant differences among the average plant water values (per treatment $n > 3$) of each sampling day are on the vertical dashed lines as letter of the treatment, for example, BC1, BC2 or C (Tukey's honestly significant difference criterion $\alpha = 0.05$).
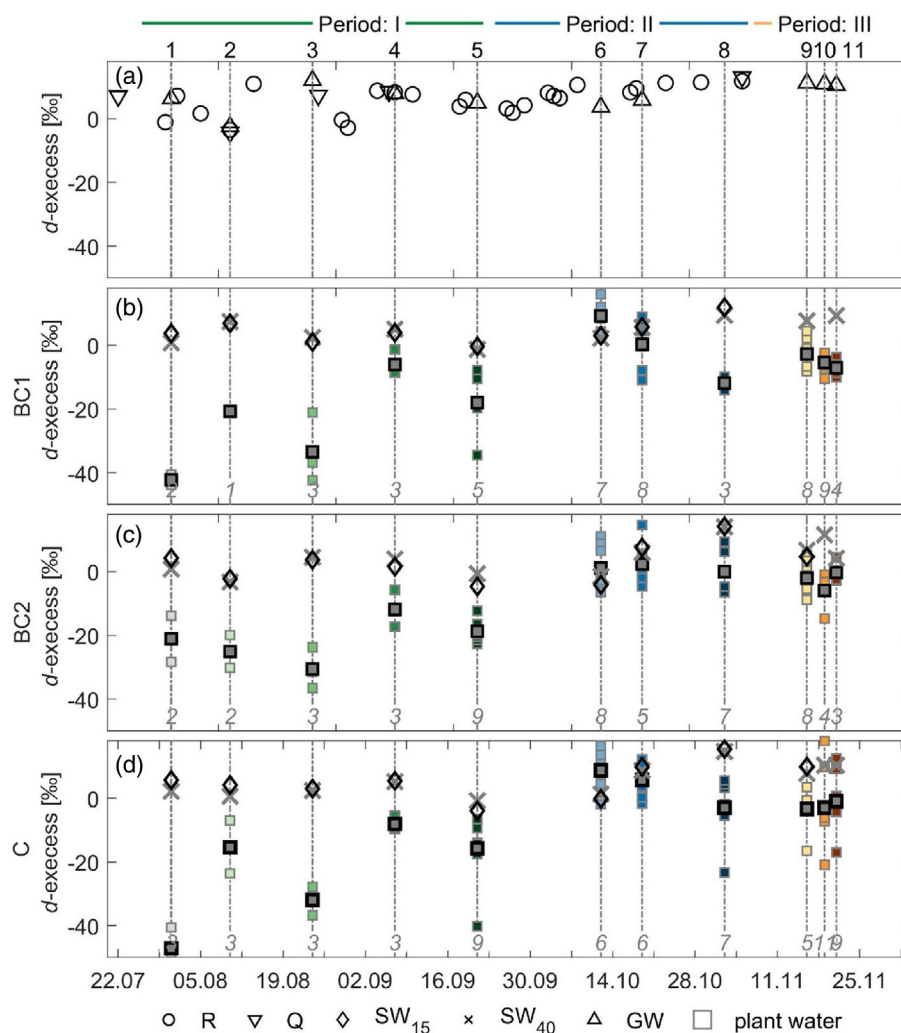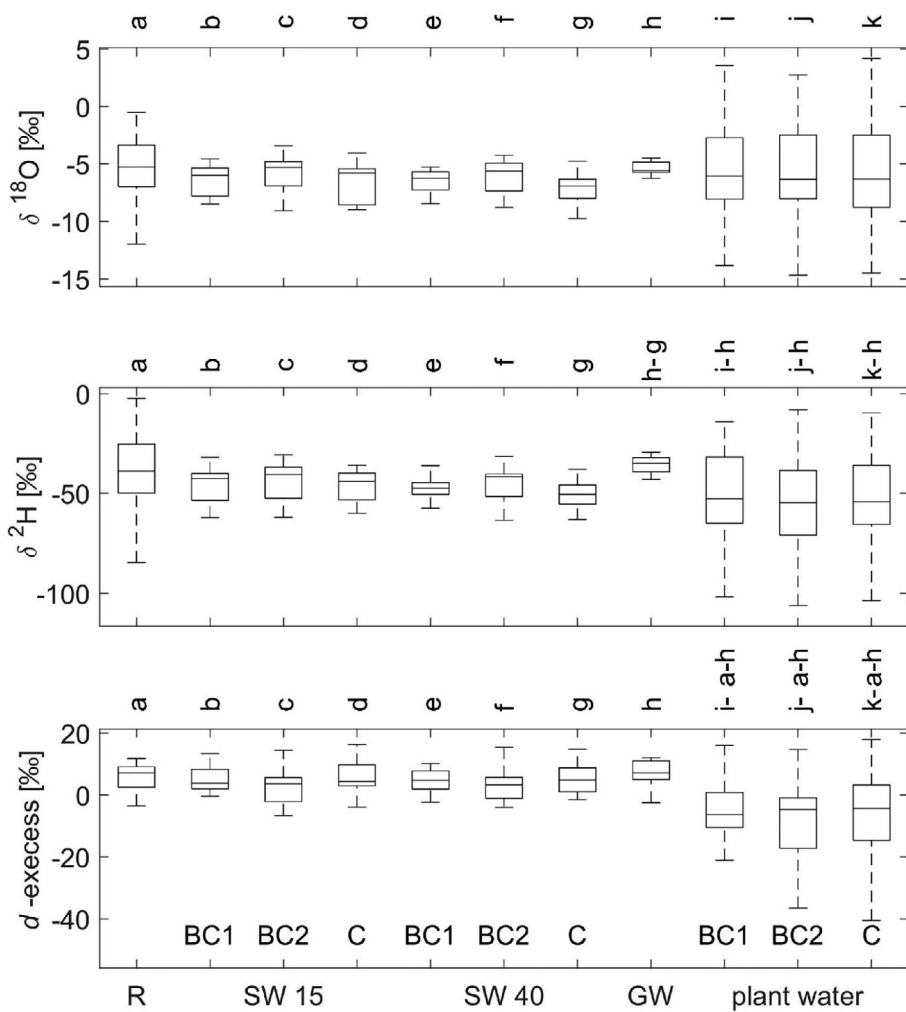
FIGURE A3 Boxplot of stable isotope composition δ^{18}O, δ^{2}H and *d-excess* of rainfall (R), mobile soil water collected at 15 cm (SW 15) and 40 cm (SW40) below surface, groundwater (GW) and plant water where BC1, BC2 and C indicate the three different treatments. The boxes show the range of values for different sample groups (showing the median and the interquartile range, with whiskers indicating 10th and 90th percentiles). Letters on top of each box indicate significant differences among the average values of the different groups (Tukey's honestly significant difference criterion α = 0.05).